

# Studies on the genus *Pyrenopolyporus* (Hypoxylaceae) in Thailand using a polyphasic taxonomic approach

Sarunyou Wongkanoun <sup>1</sup>, Boonchuai Chainuwong <sup>1</sup>, Noppol Kobmoo <sup>2</sup>, Sittiruk Roytrakul <sup>3</sup>, Sayanh Somrithipol <sup>2</sup>, Jennifer Luangsa-ard <sup>2</sup>, Esteban Charria-Girón <sup>4,5</sup>, Prasert Srikitikulchai <sup>1,\*</sup> and Marc Stadler <sup>4,5,\*</sup>

<sup>1</sup> National Biobank of Thailand (NBT), National Science and Technology Development Agency (NSTDA), 111 Thailand Science Park, Phahonyothin Road, Khlong Nueng, Khlong Luang, Pathum Thani 12120, Thailand; sarunyou.won@nstda.or.th (S.W.)

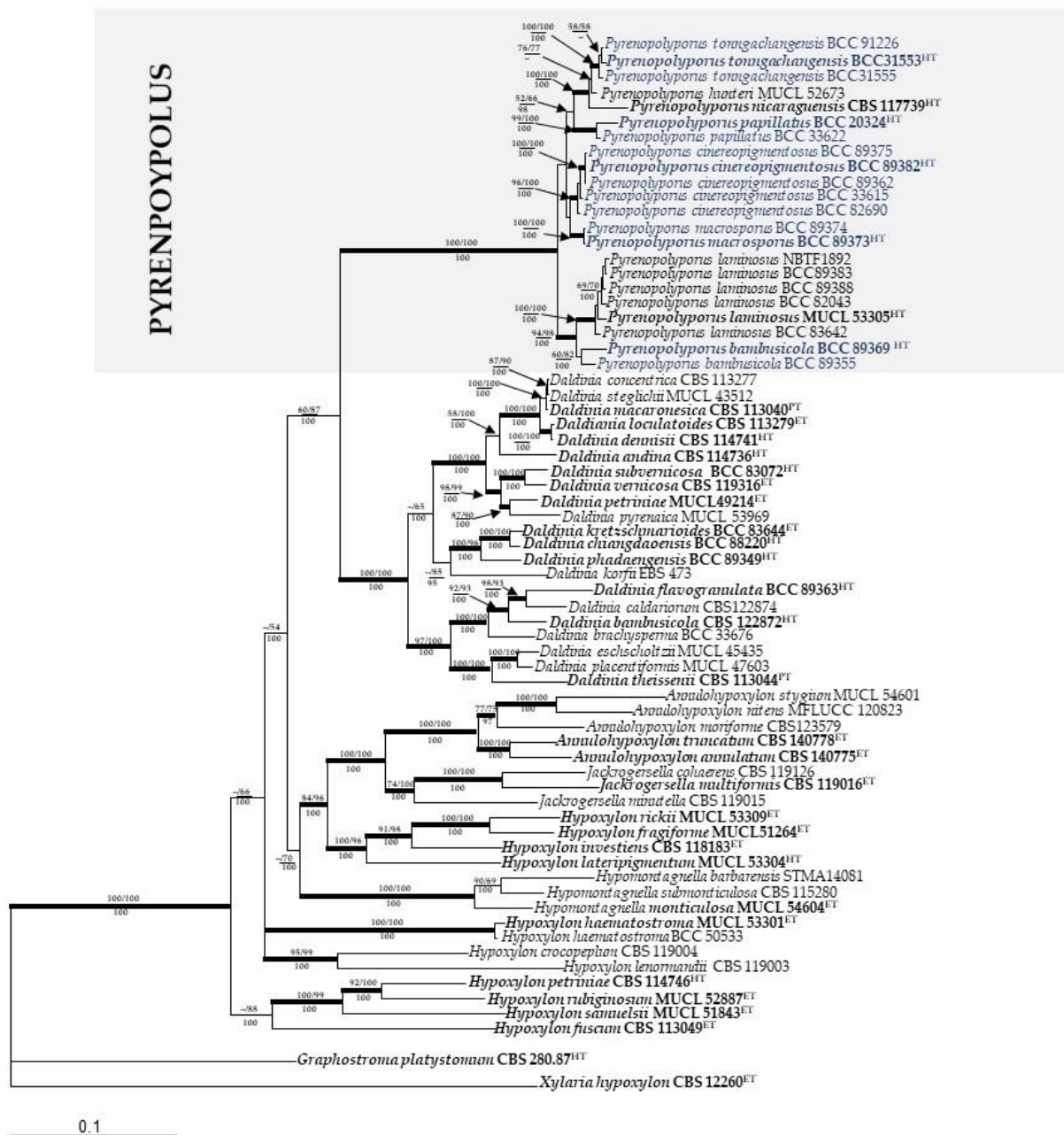
<sup>2</sup> Plant Microbe Interaction Research Team (APMT), Integrative Crop Biotechnology and Management Research Group, National Center for Genetic Engineering and Biotechnology (BIOTEC), 113 Thailand Science Park, Phahonyothin Road, Khlong Nueng, Khlong Luang, Pathum Thani 12120, Thailand; noppol.kob@biotec.or.th (N.K.)

<sup>3</sup> Functional Proteomics Technology (IFPT), Functional Ingredients and Food Innovation Research Group, National Center for Genetic Engineering and Biotechnology, 113 Thailand Science Park, Phahonyothin Road, Khlong Nueng, Khlong Luang 12120, Pathum Thani, Thailand

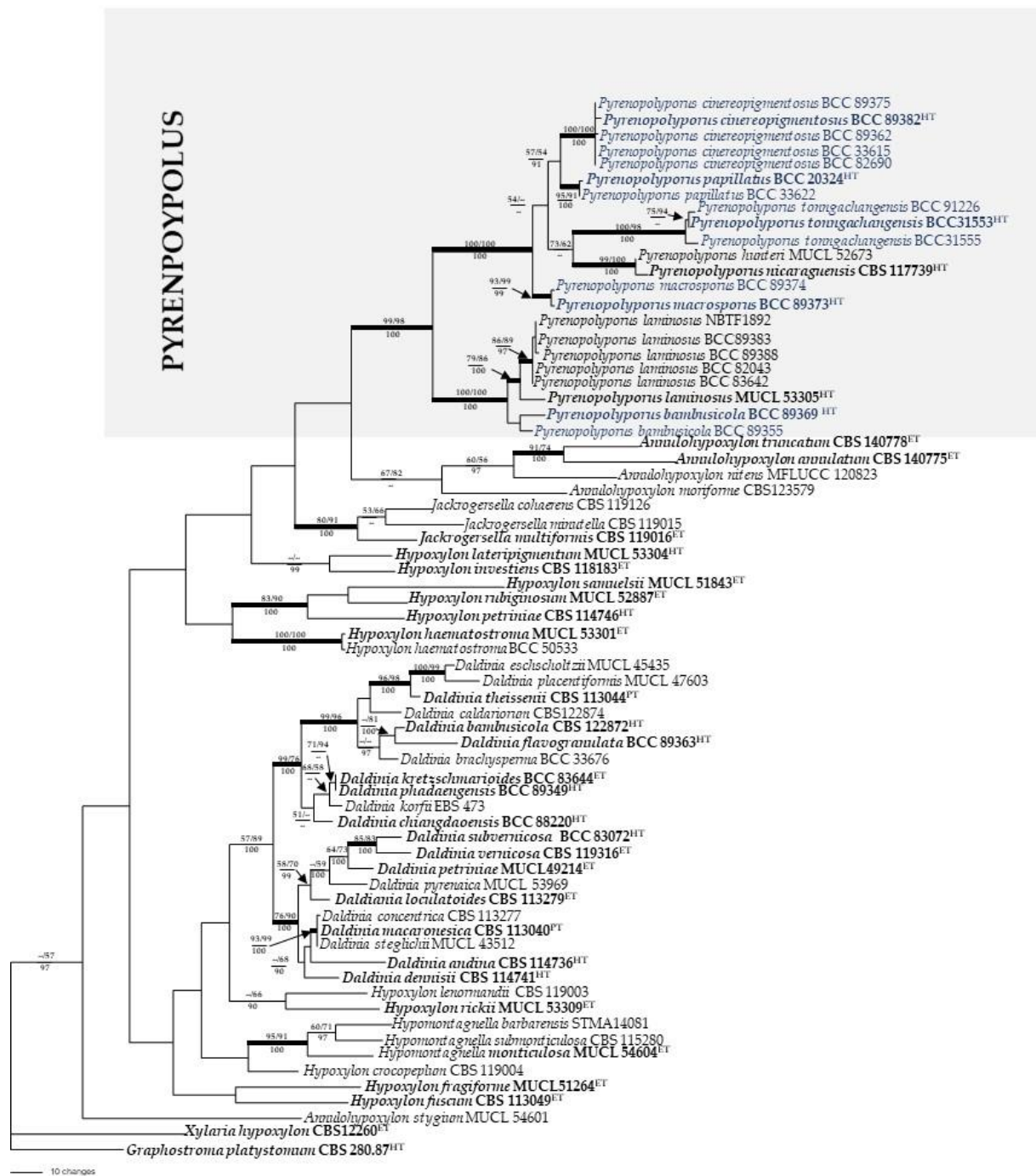
<sup>4</sup> Department of Microbial Drugs, Helmholtz Centre for Infection Research GmbH (HZI), and German Centre for Infection Research Association (DZIF), Hannover-Braunschweig, Inhoffenstraße 7, Braunschweig 38124, Germany

<sup>5</sup> Institute of Microbiology, Technische Universität Braunschweig, Spielmannstraße 7, Braunschweig 38106, Germany

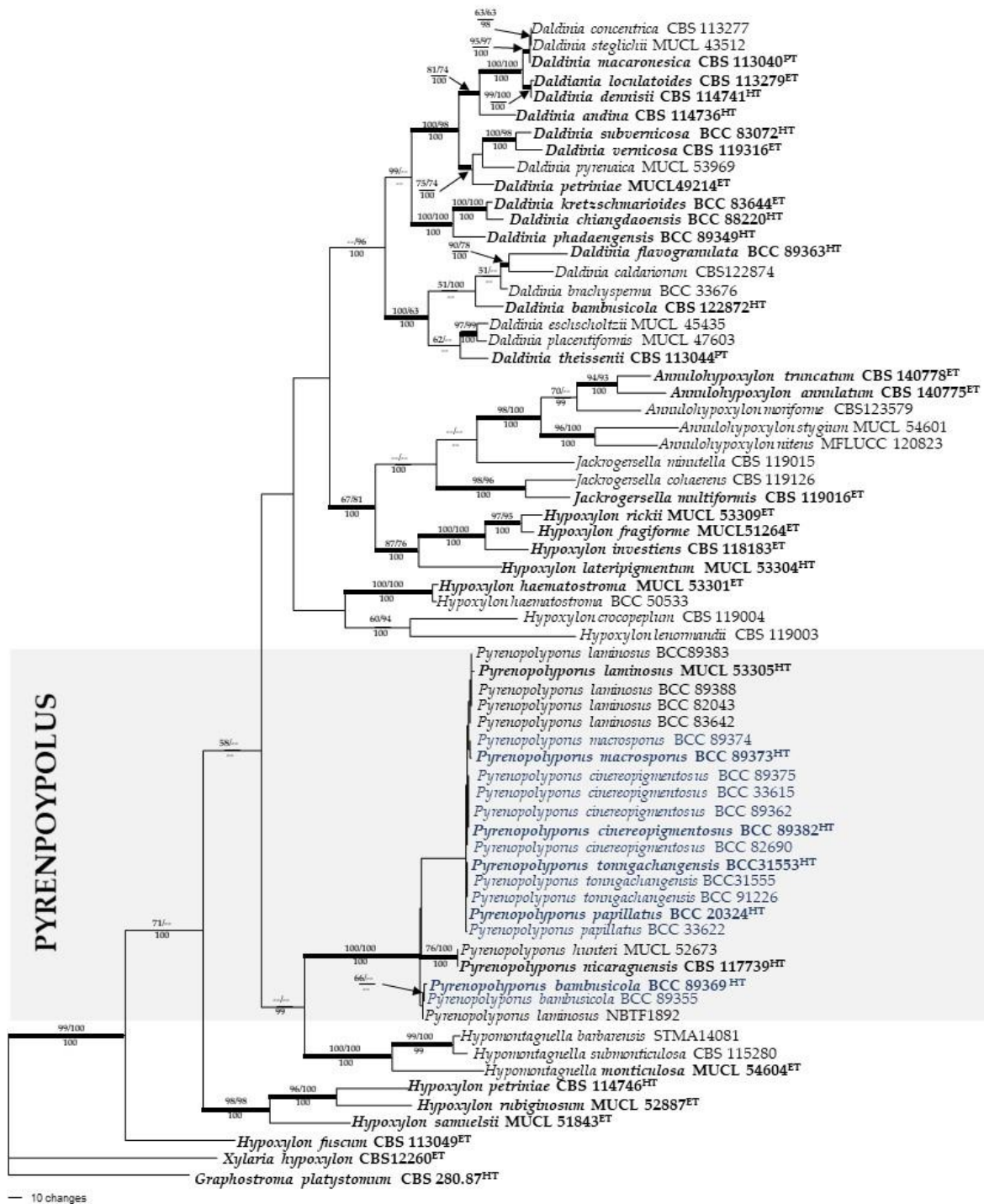
\* Correspondence: prasert@nstda.or.th (P.S.); marc.stadler@helmholtz-hzi.de (M.S.)



**Figure S1.** Phylogeny of the Hypoxylaceae. The phylogenetic relationships inferred from Bayesian analysis based on multiple genetic loci of nuclear ribosomal LSU and proteinogenic (*TUB2* and *RPB2*) sequences. Support values of more than 50% (MPBS/MLBS) or 0.95 (BPP) were calculated via MP, ML and Bayesian analysis and are indicated above (MPBS/MLBS) and below (BPP) the respective branches. Branches of significant support (MPBS, MLBS =70% and BPP =95) are thickened. New species are indicated in blue and the clade comprising the sequences of the *Pyrenopezizomycetes* spp. is marked by a grey rectangle, ET indicates ex-epitype, HT ex-holotype, and PT ex-paratype strains.

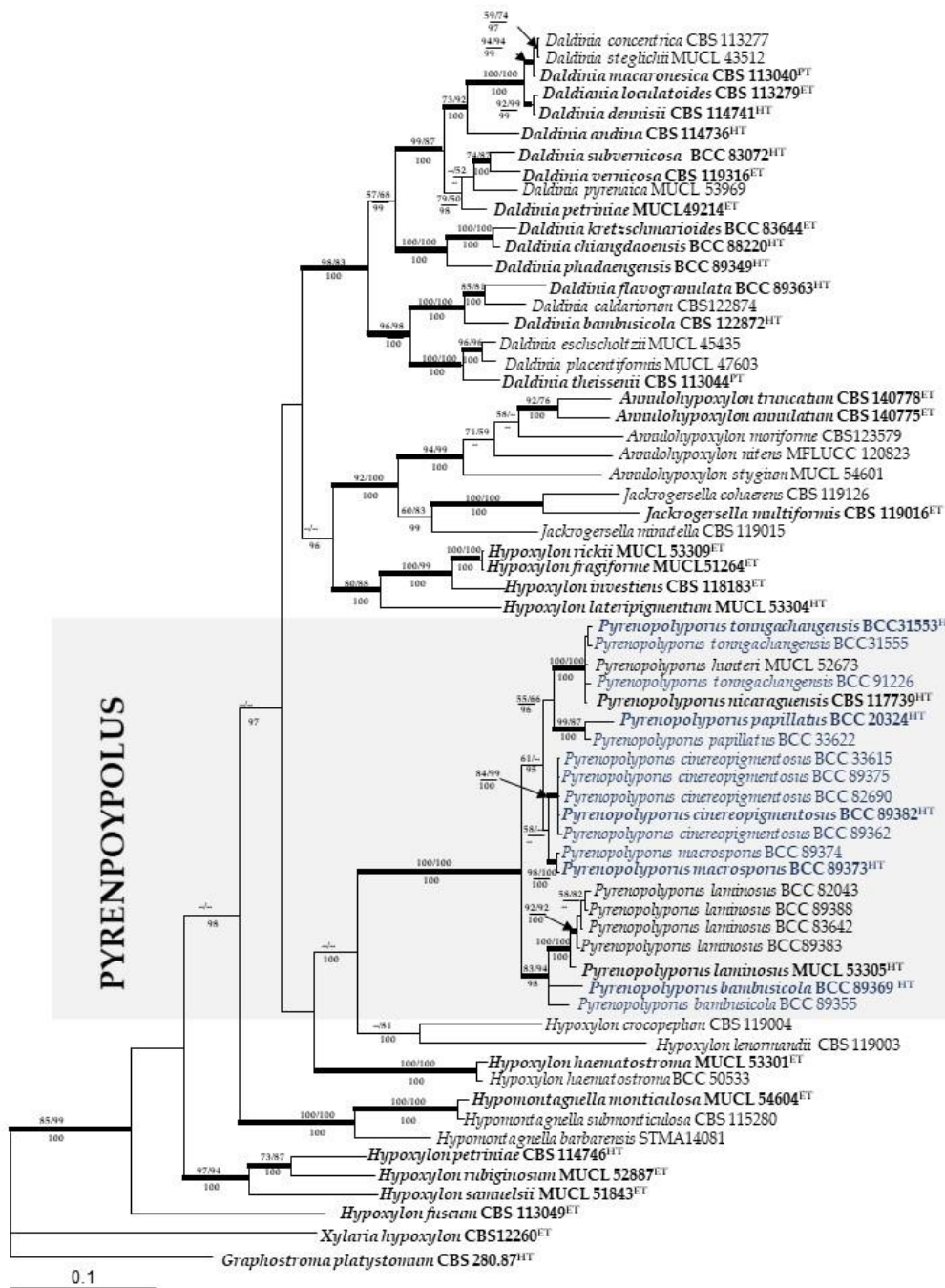


**Figure S2.** Phylogeny of the Hypoxylaceae. The phylogenetic relationships depicted as Maximum parsimony tree generated based on ITS sequences. Support values of more than 50% (MPBS/MLBS) or 95 (BPP) were calculated via MP, ML and Bayesian analysis and are indicated above (MPBS/MLBS) and below (BPP) the respective branches. Branches of significant support (MPBS, MLBS = 70% and BPP = 95) are thickened. New species are indicated in blue and the clade comprising the sequences of the *Pyrenopeziza* spp. is marked by a grey rectangle, ET indicates ex-epitype, HT ex-holotype, and PT ex-paratype strains.

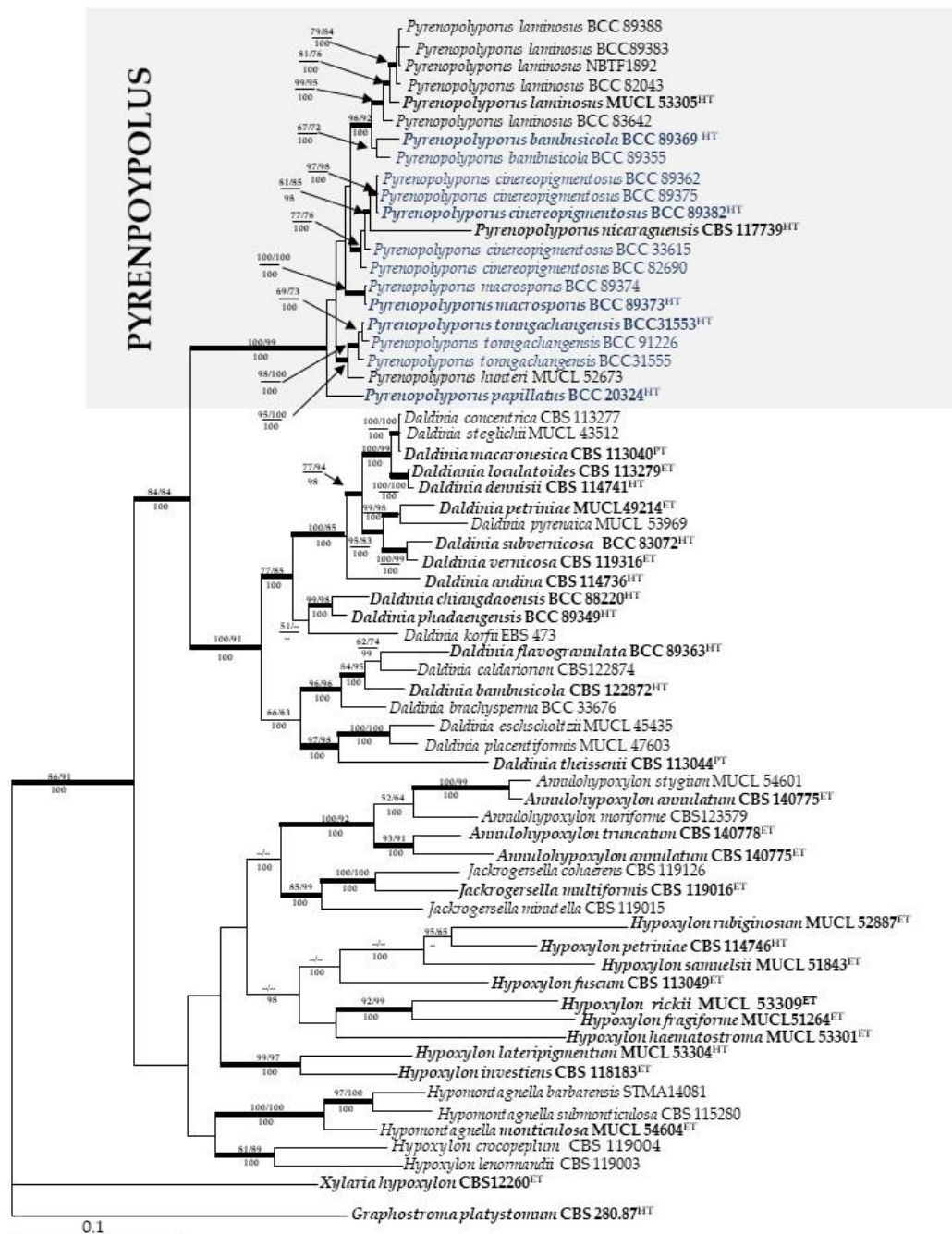


**Figure S3.** Phylogeny of the Hypoxylaceae. The phylogenetic relationships depicted as Maximum parsimony tree generated based on LSU sequences. Support values of more than 50% (MPBS/MLBS) or 95 (BPP) were calculated via MP, ML and Bayesian analysis and are indicated above (MPBS/MLBS) and below (BPP) the respective branches. Branches of significant support (MPBS, MLBS =70% and BPP =95) are thickened. New species are indicated in blue and the clade comprising the sequences of the *Pyrenopeziza* spp. is marked by a grey rectangle, ET indicates ex-epitype, HT ex-holotype, and PT ex-paratype strains.

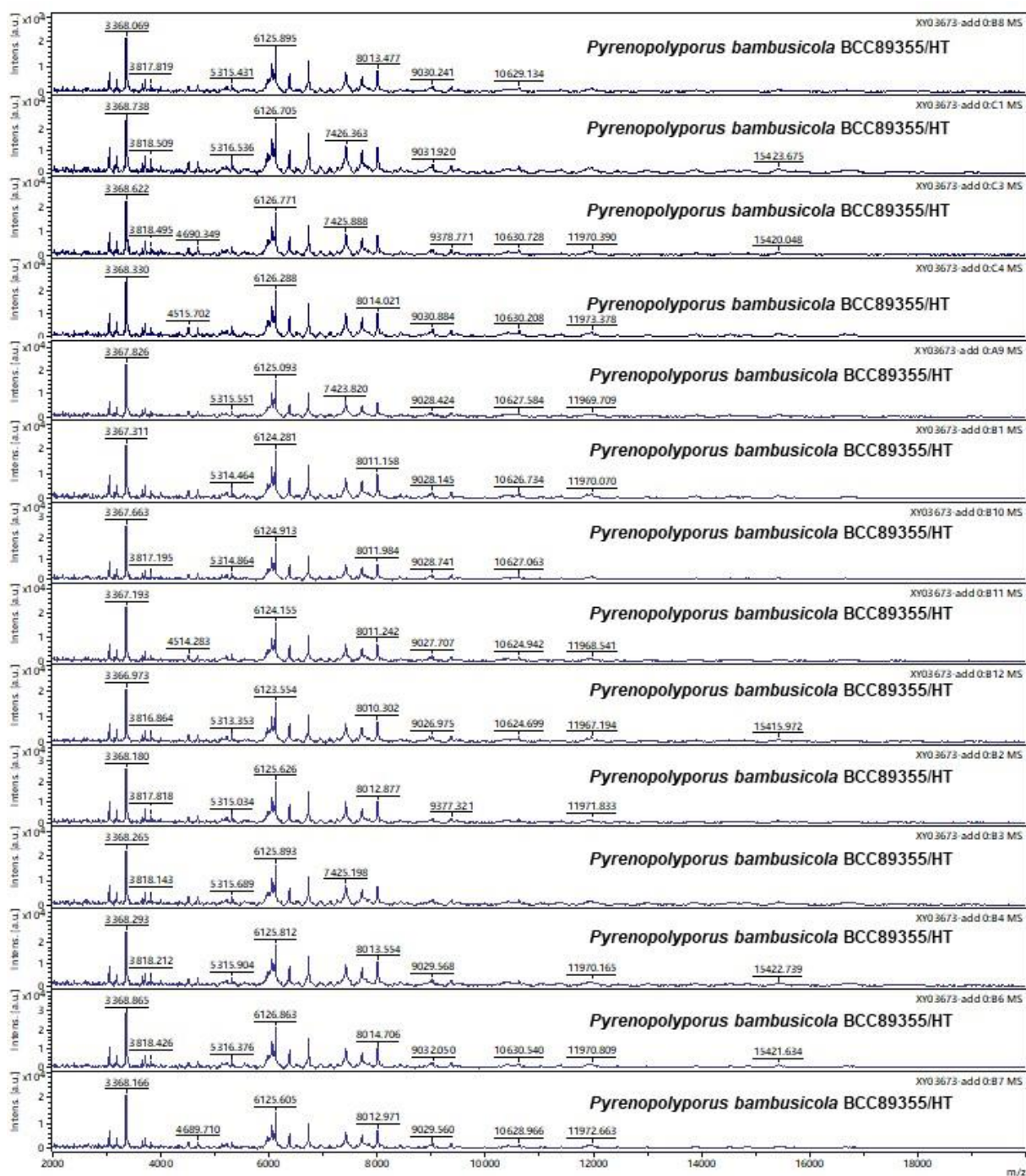




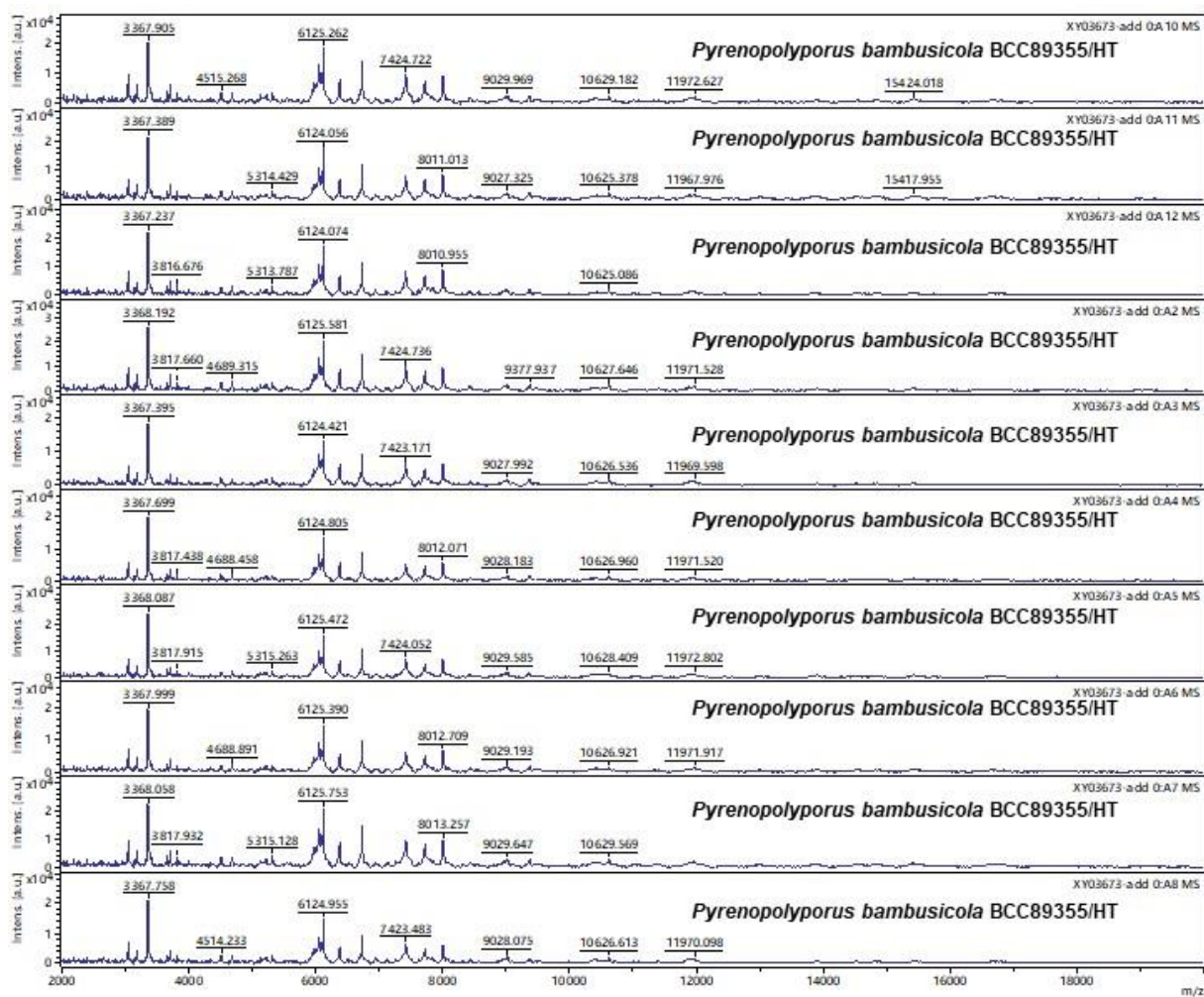
**Figure S4.** Phylogeny of the Hypoxylaceae. The phylogenetic relationships inferred from Bayesian analysis based on proteinogenic (*RPB2*) sequences. Support values of more than 50% (MPBS/MLBS) or 0.95 (BPP) were calculated via MP, ML and Bayesian analysis and are indicated above (MPBS/MLBS) and below (BPP) the respective branches. Branches of significant support (MPBS, MLBS =70% and BPP =95) are thickened. New species are indicated in blue and the clade comprising the sequences of the *Pyrenopeziza* spp. is marked by a grey rectangle, ET indicates ex-epitype, HT ex-holotype, and PT ex-paratype strains.



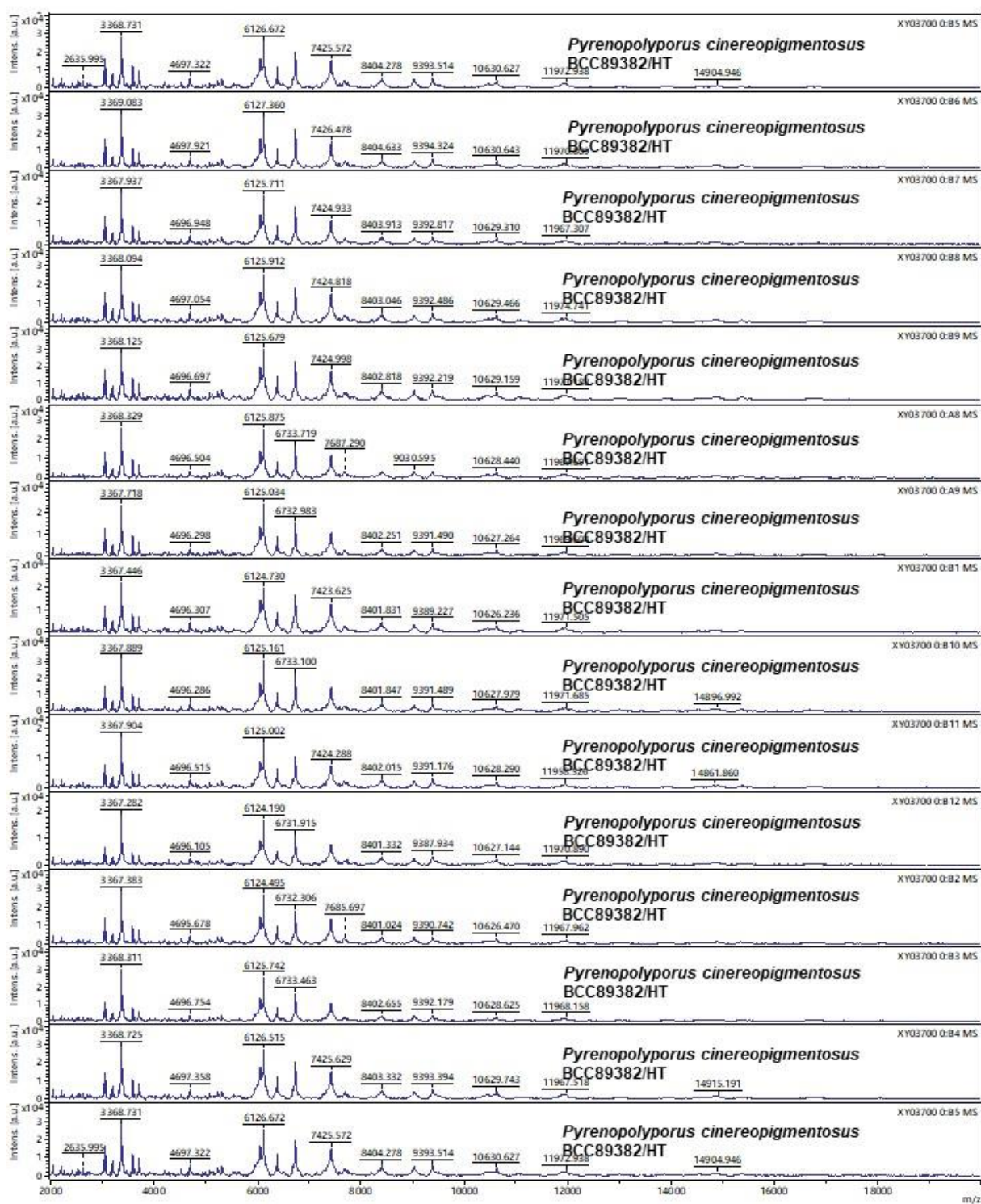
**Figure S5.** Phylogeny of the Hypoxylaceae. The phylogenetic relationships inferred from Bayesian analysis based on proteinogenic (*TUB2*) sequences. Support values of more than 50% (MPBS/MLBS) or 0.95 (BPP) were calculated via MP, ML and Bayesian analysis and are indicated above (MPBS/MLBS) and below (BPP) the respective branches. Branches of significant support (MPBS, MLBS = 70% and BPP = 95) are thickened. New species are indicated in blue and the clade comprising the sequences of the *Pyrenopezizomycetes* spp. is marked by a grey rectangle, ET indicates ex-epitype, HT ex-holotype, and PT ex-paratype strains.

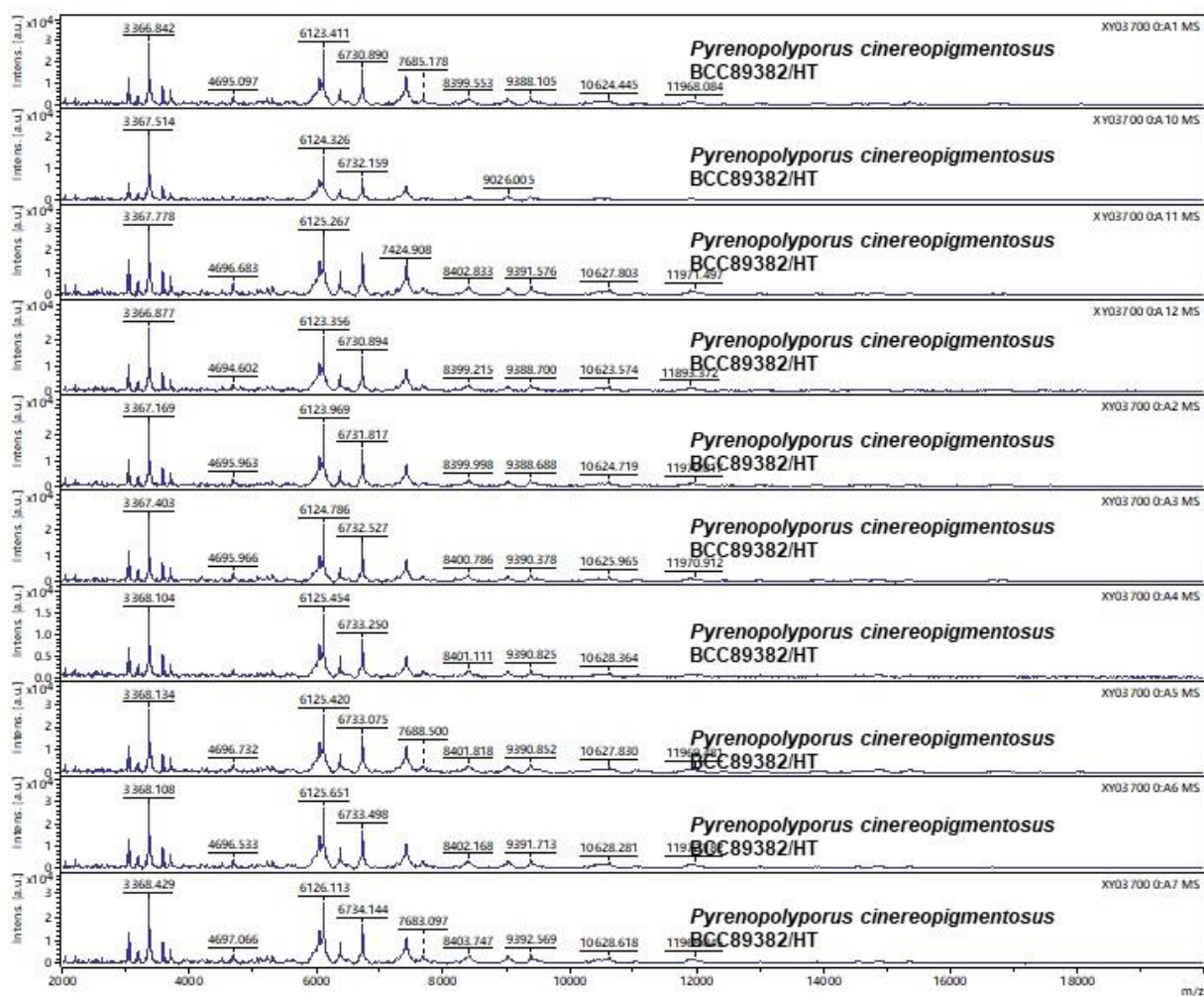


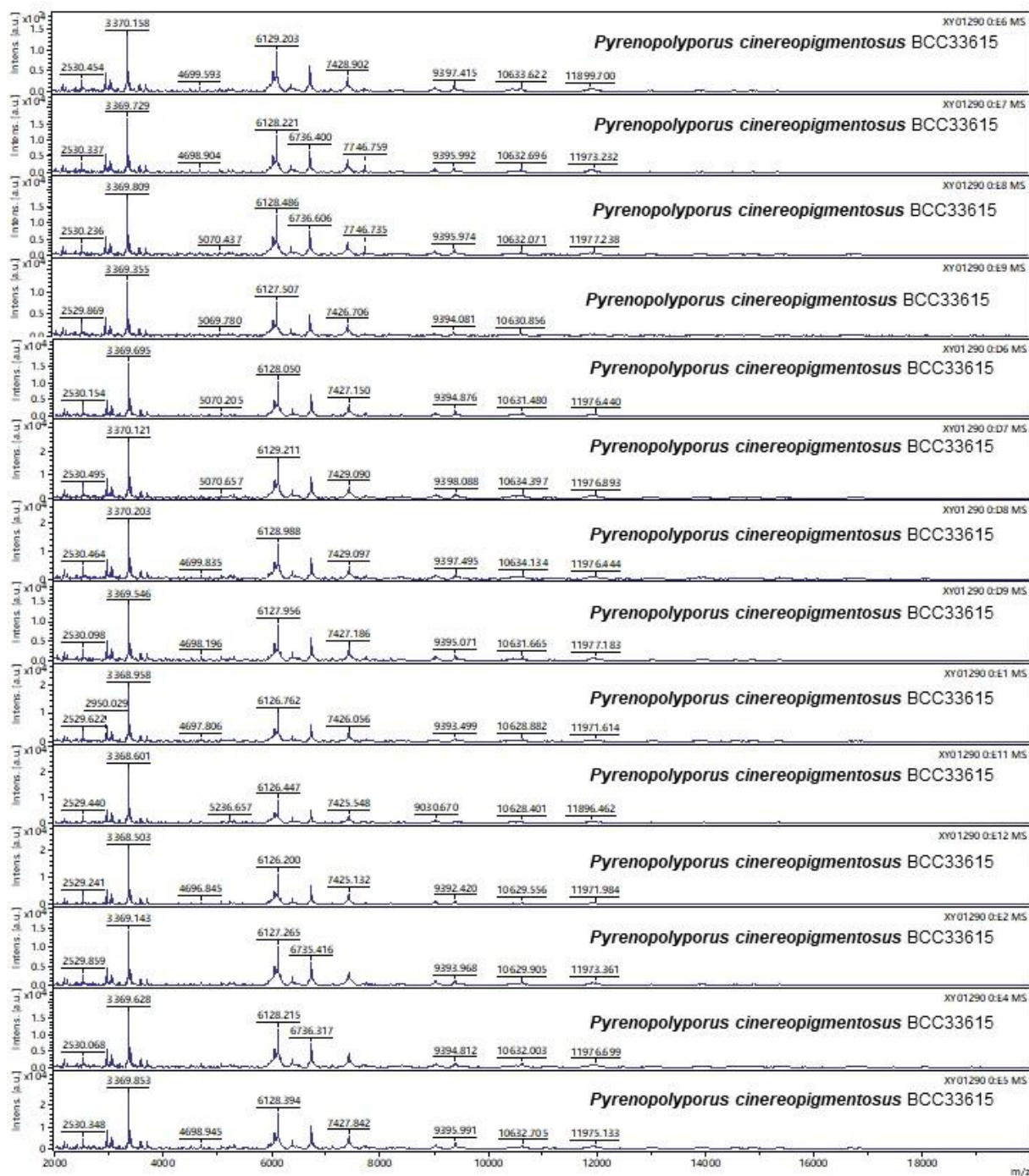




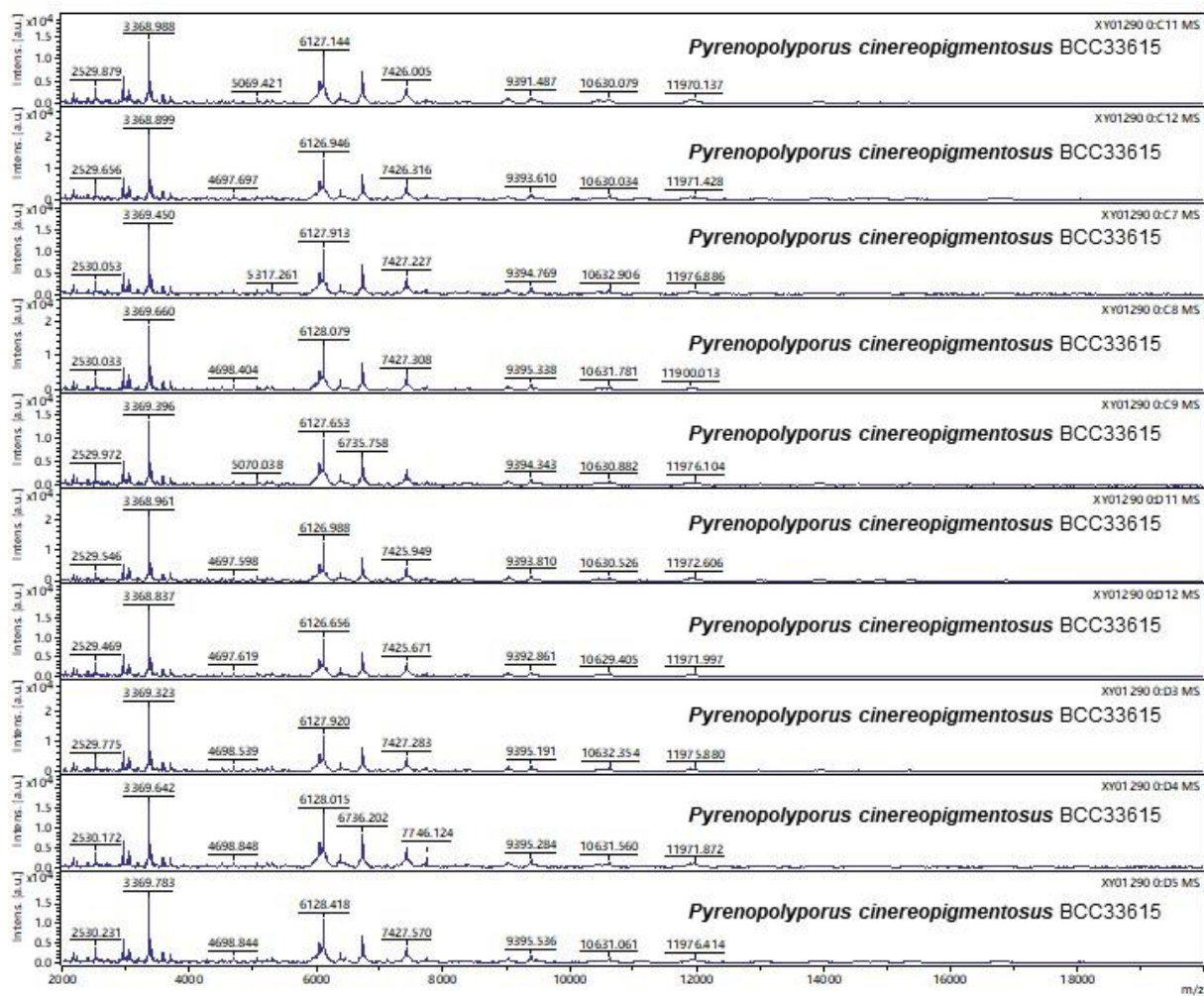


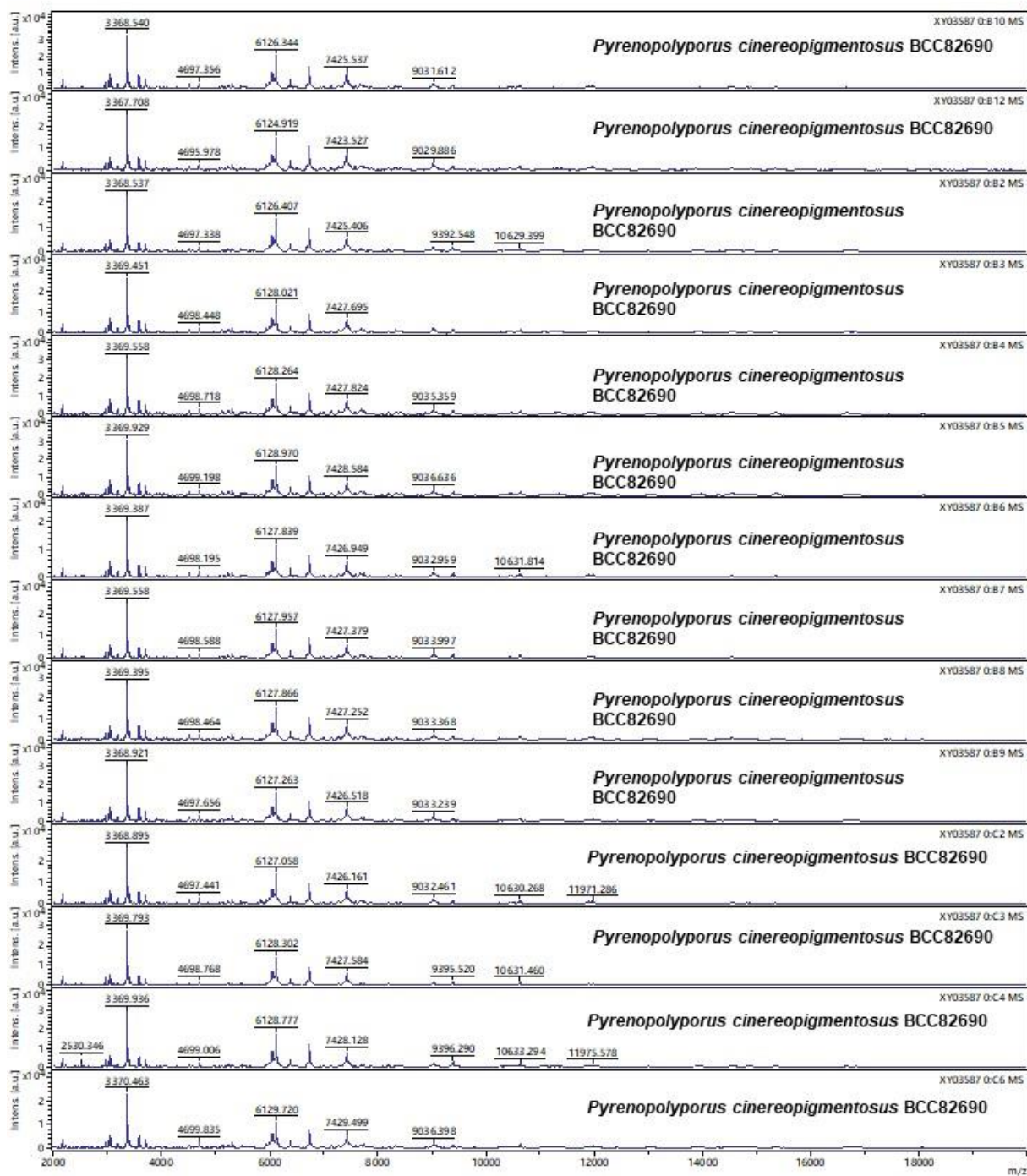


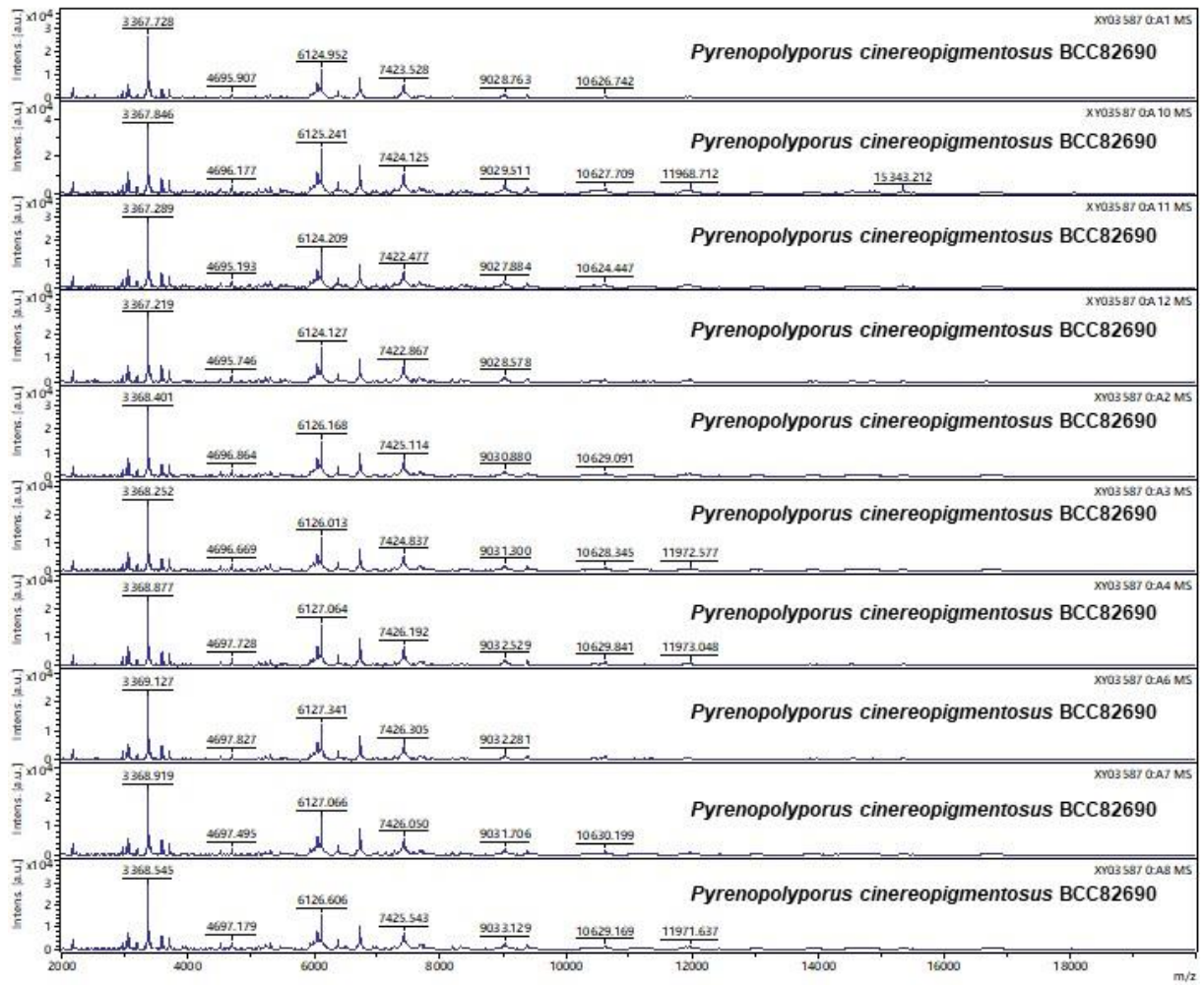




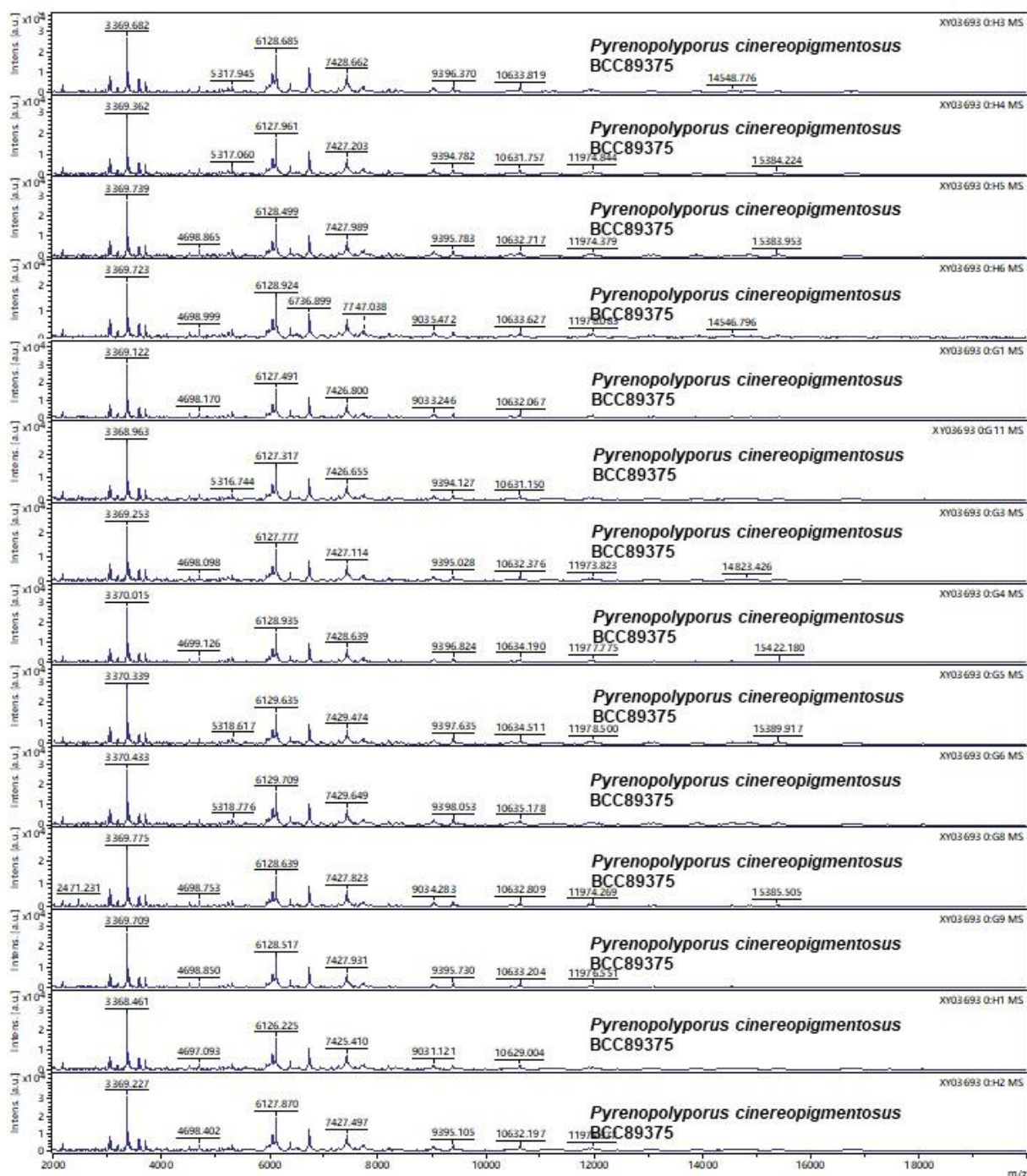


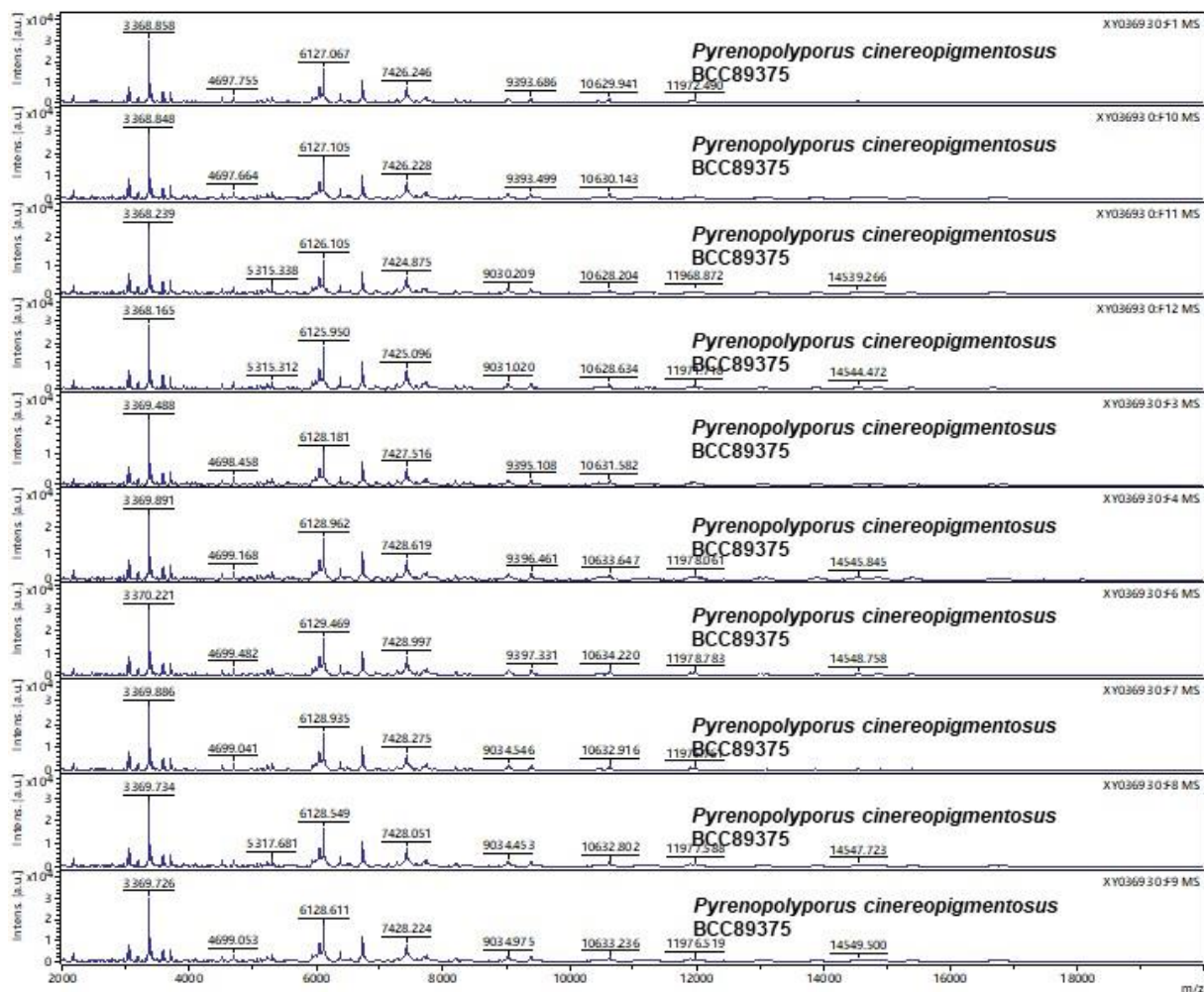


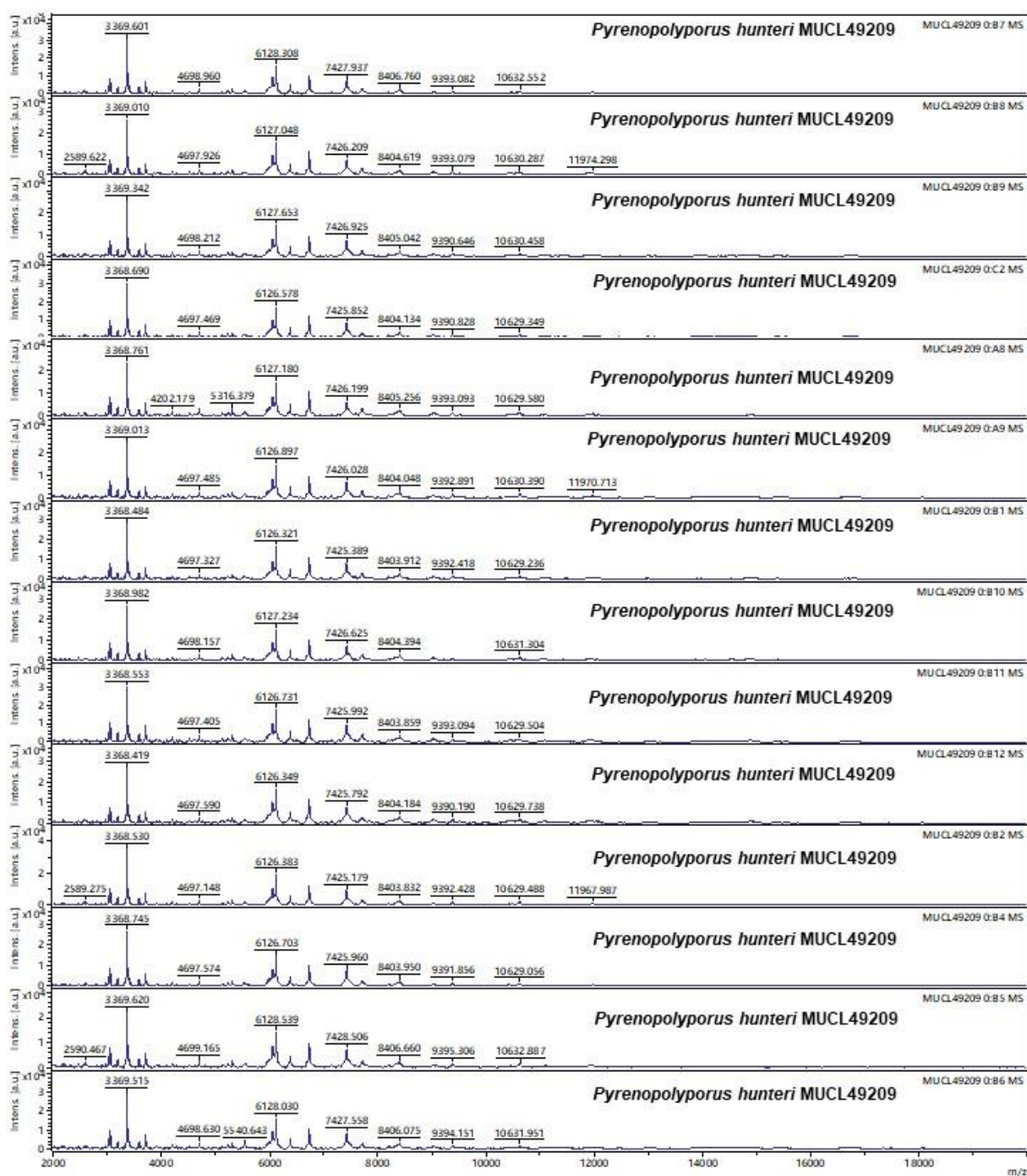




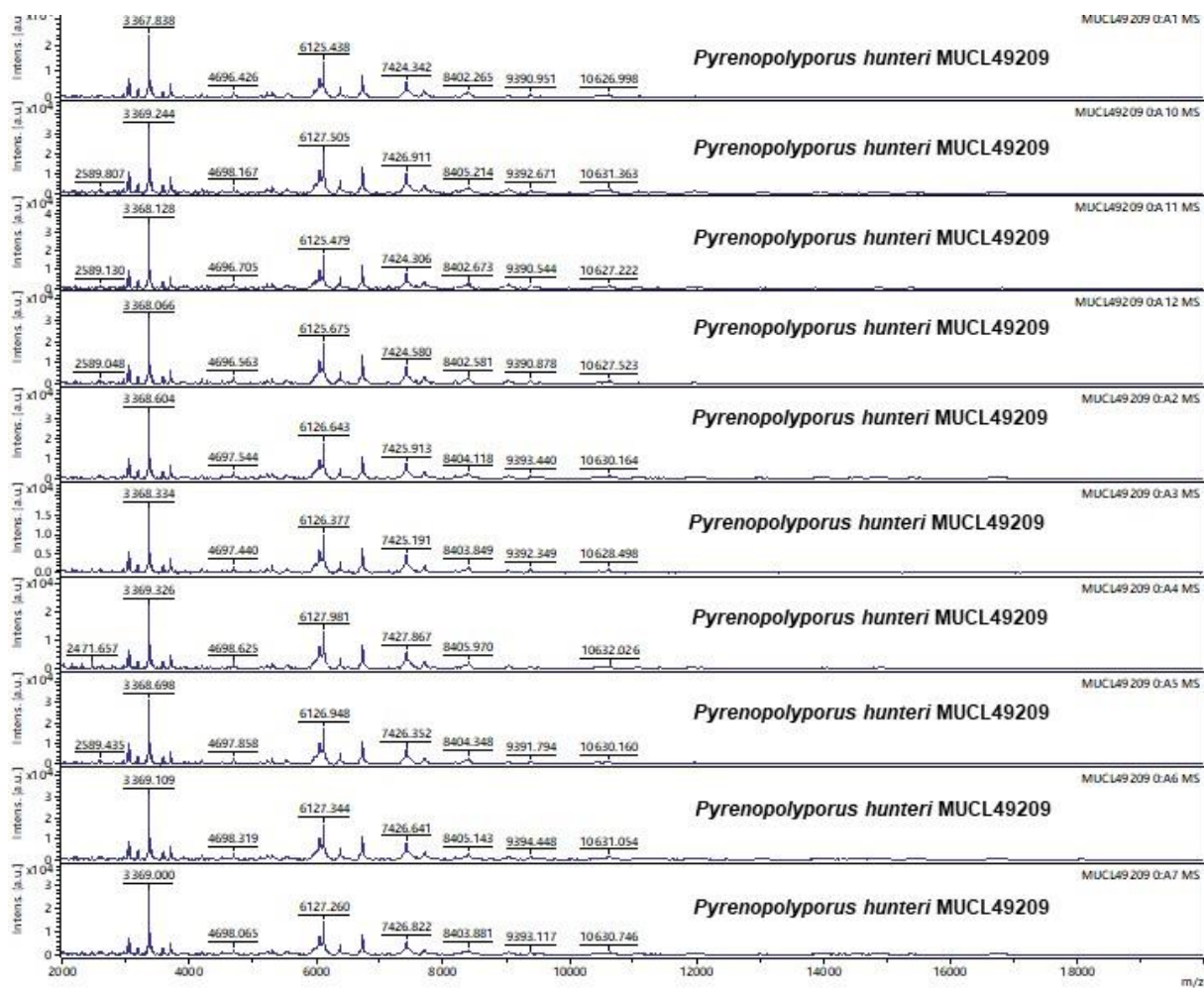


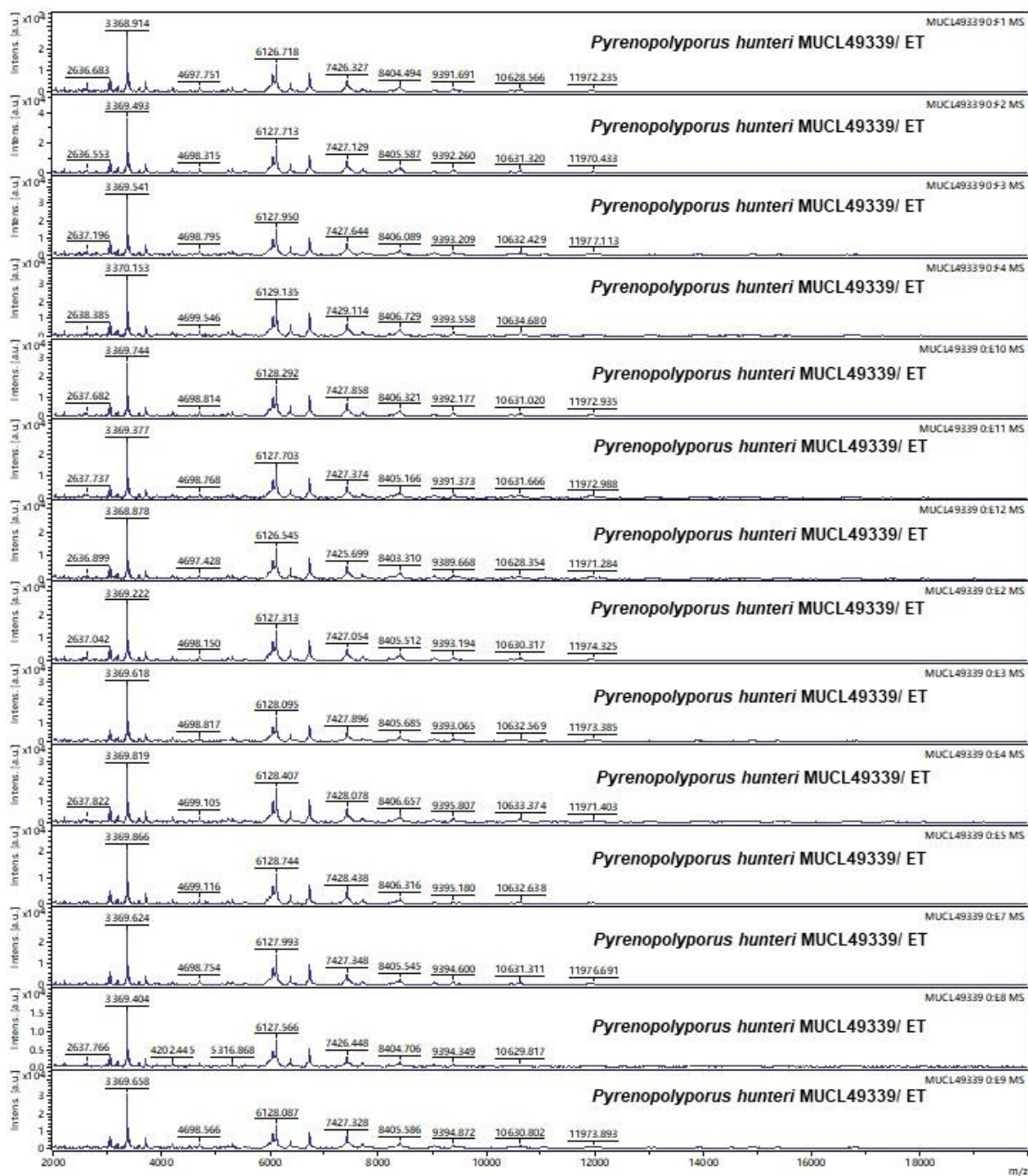


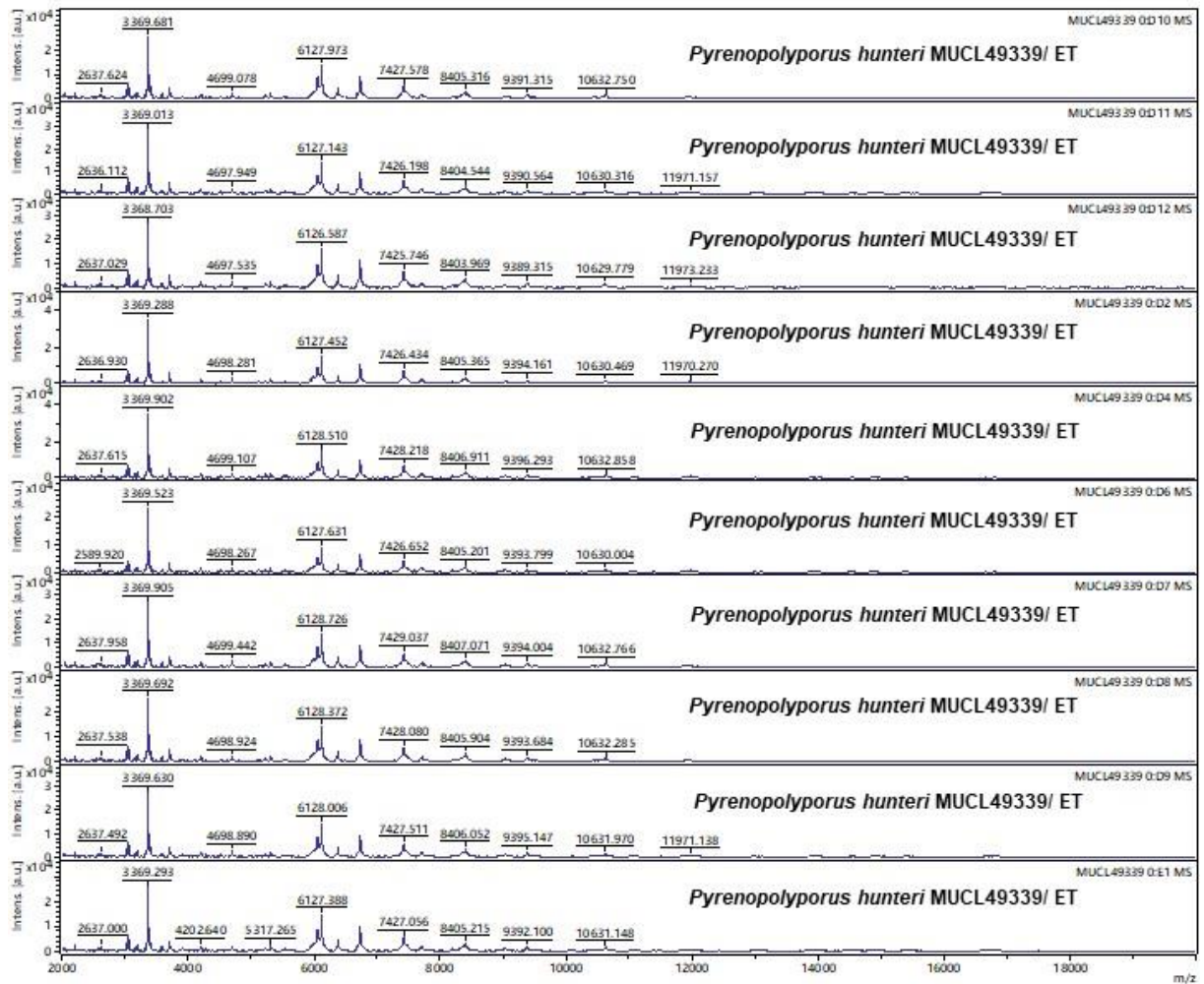




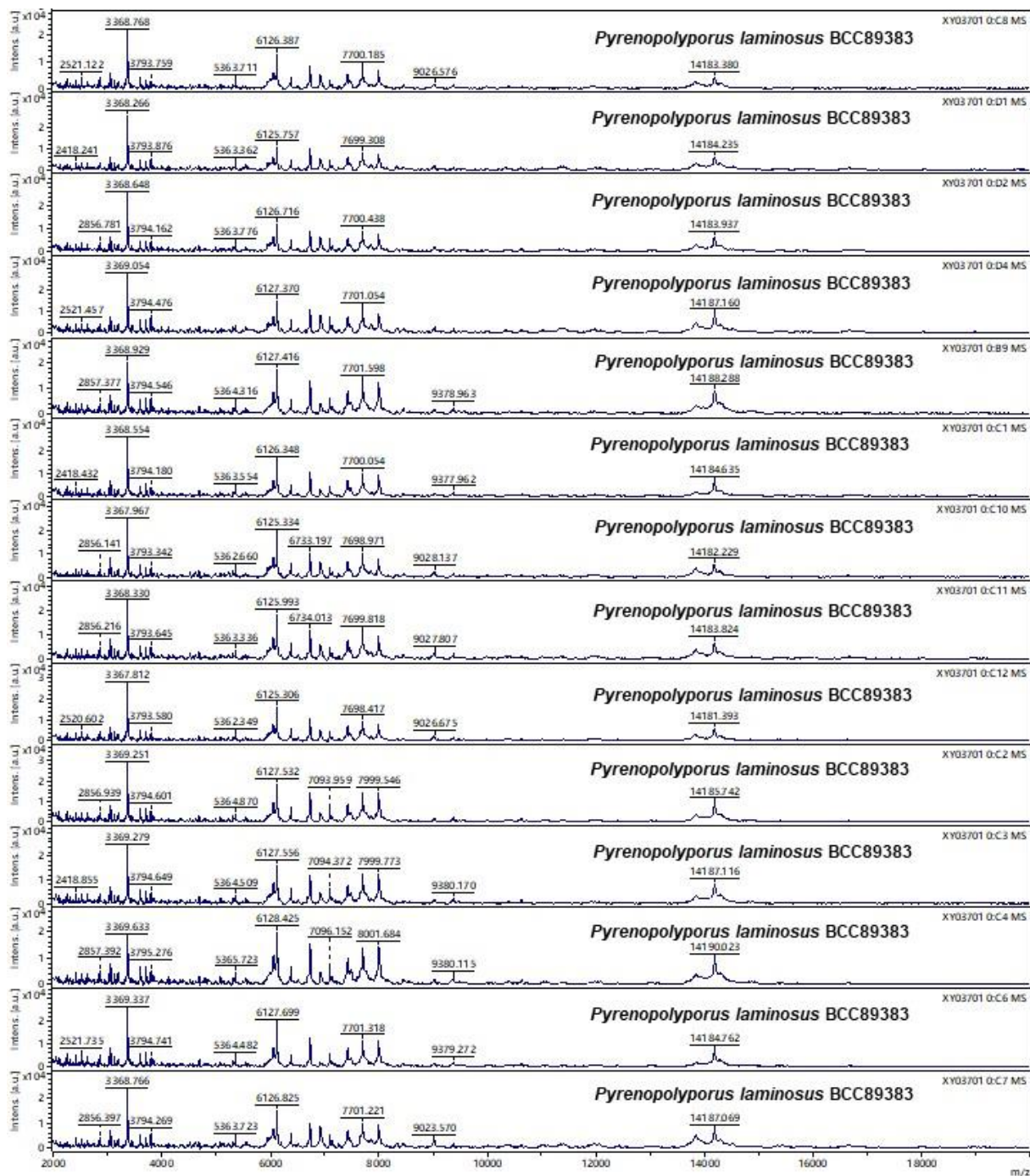


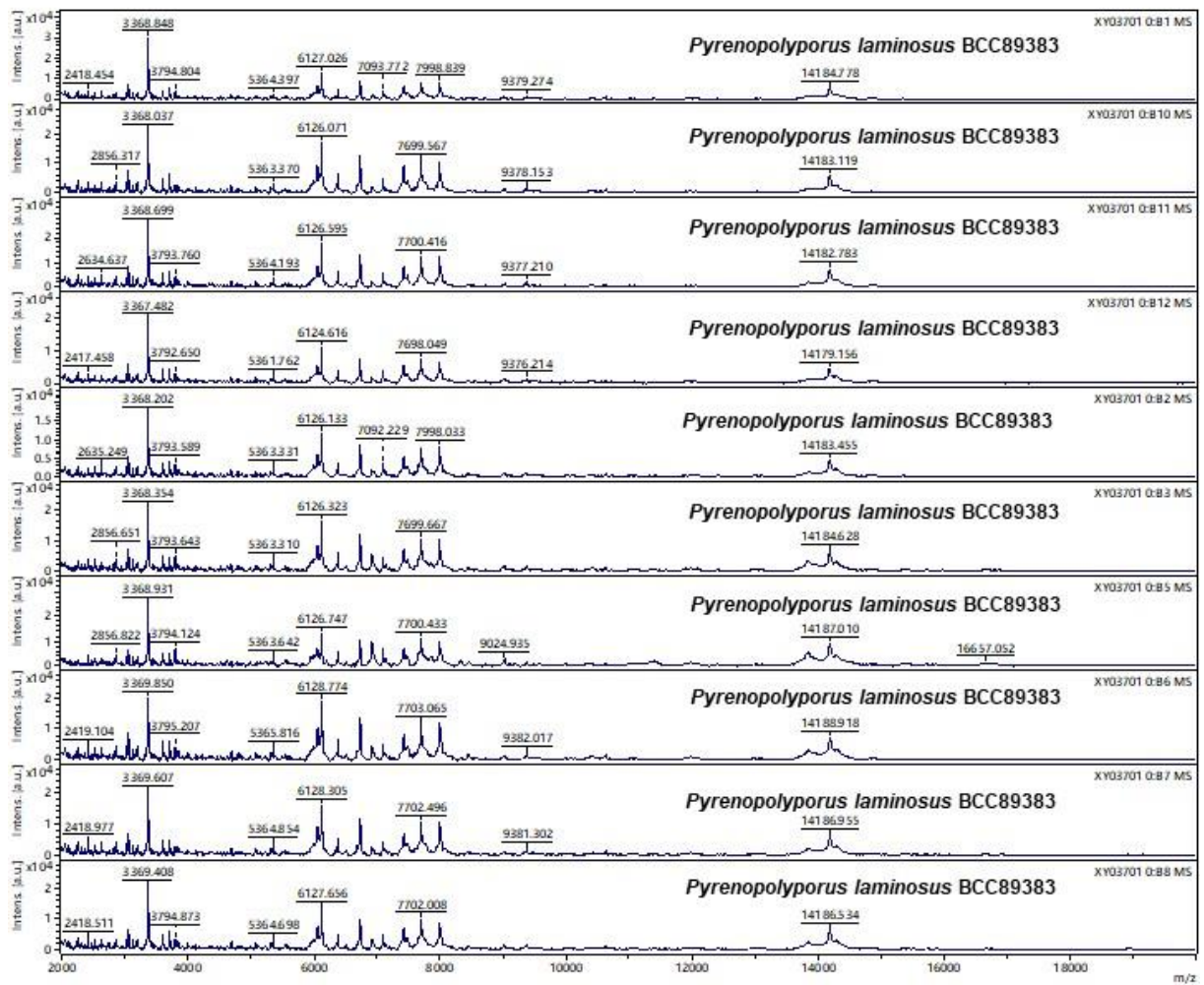


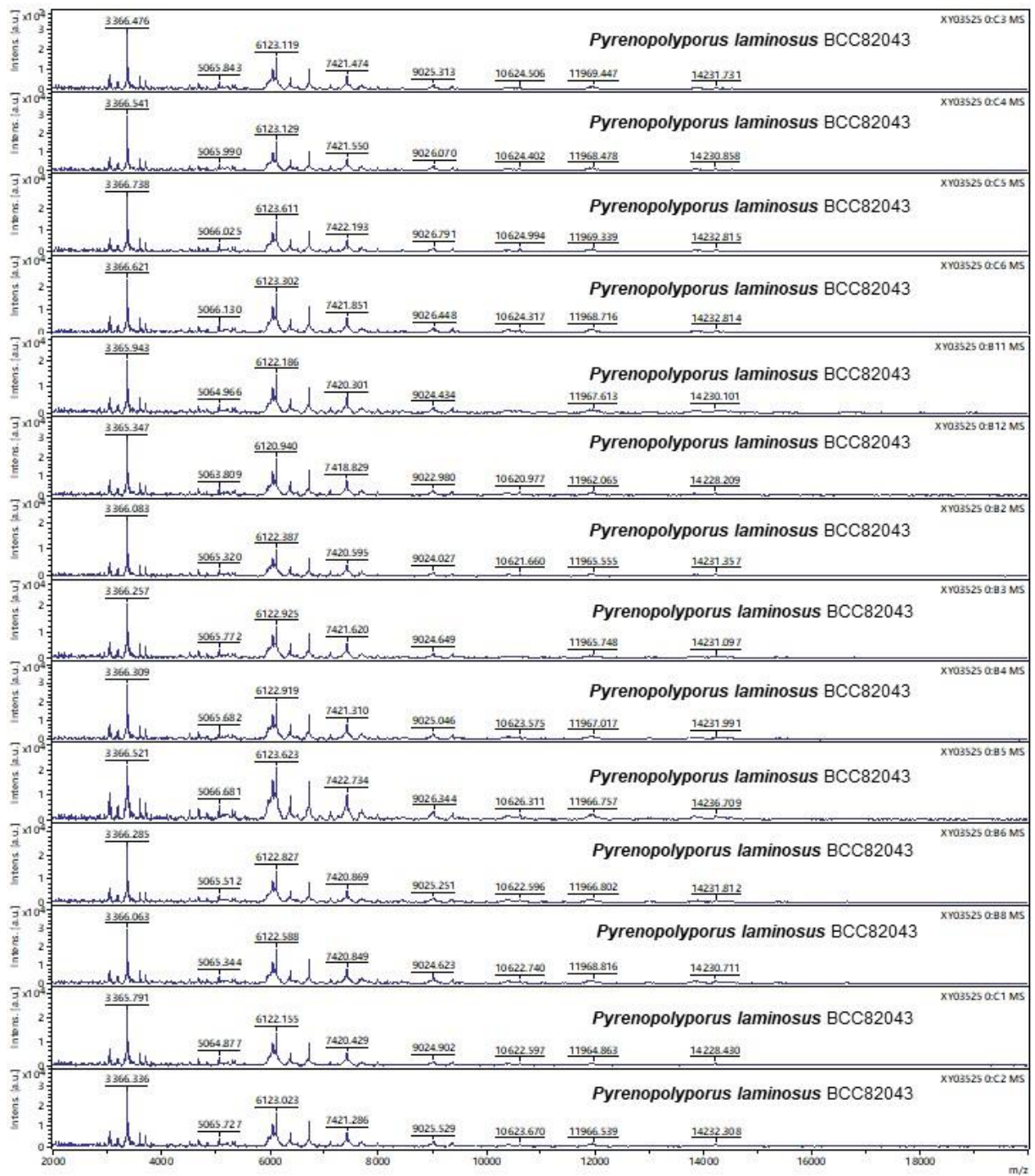




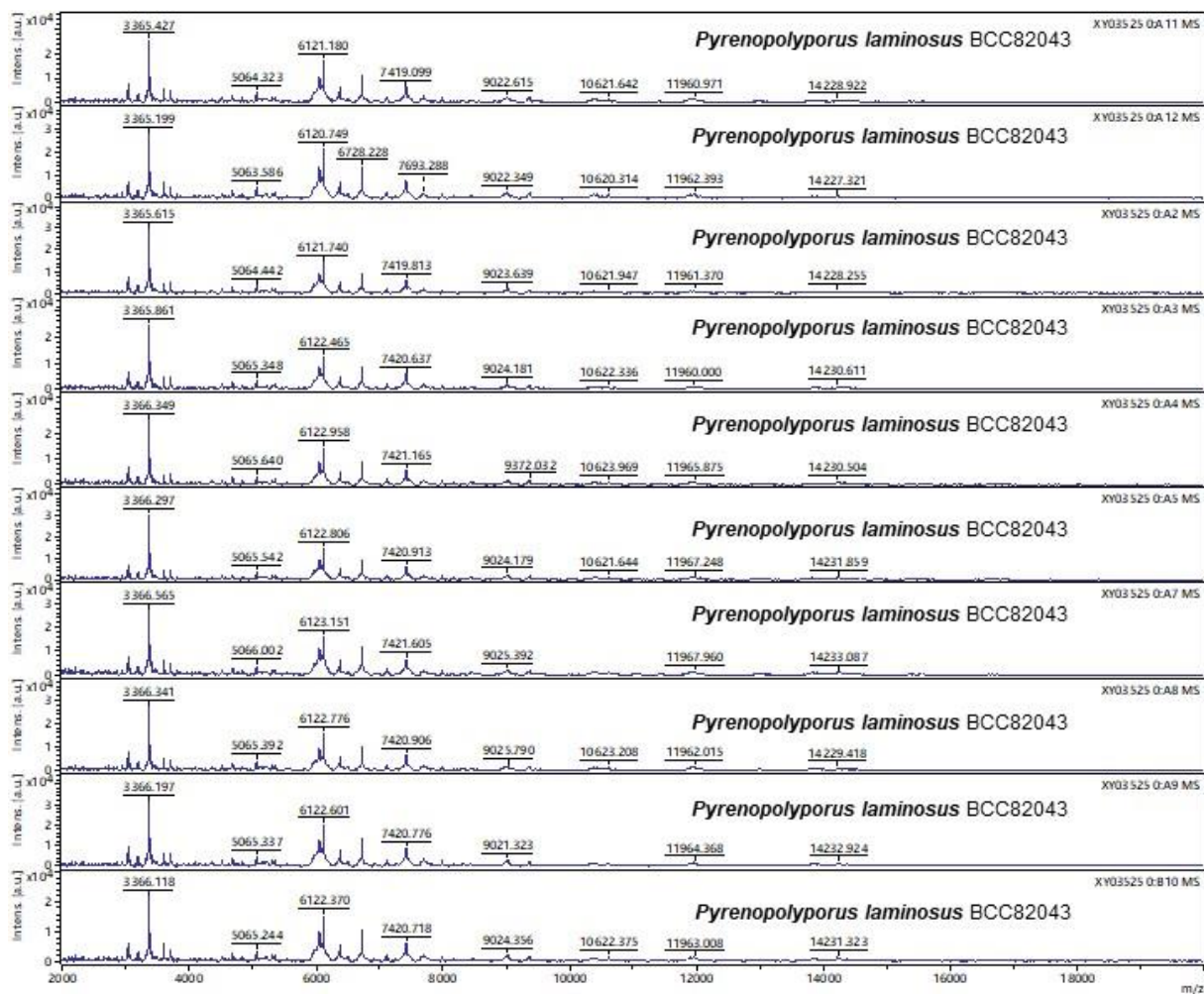


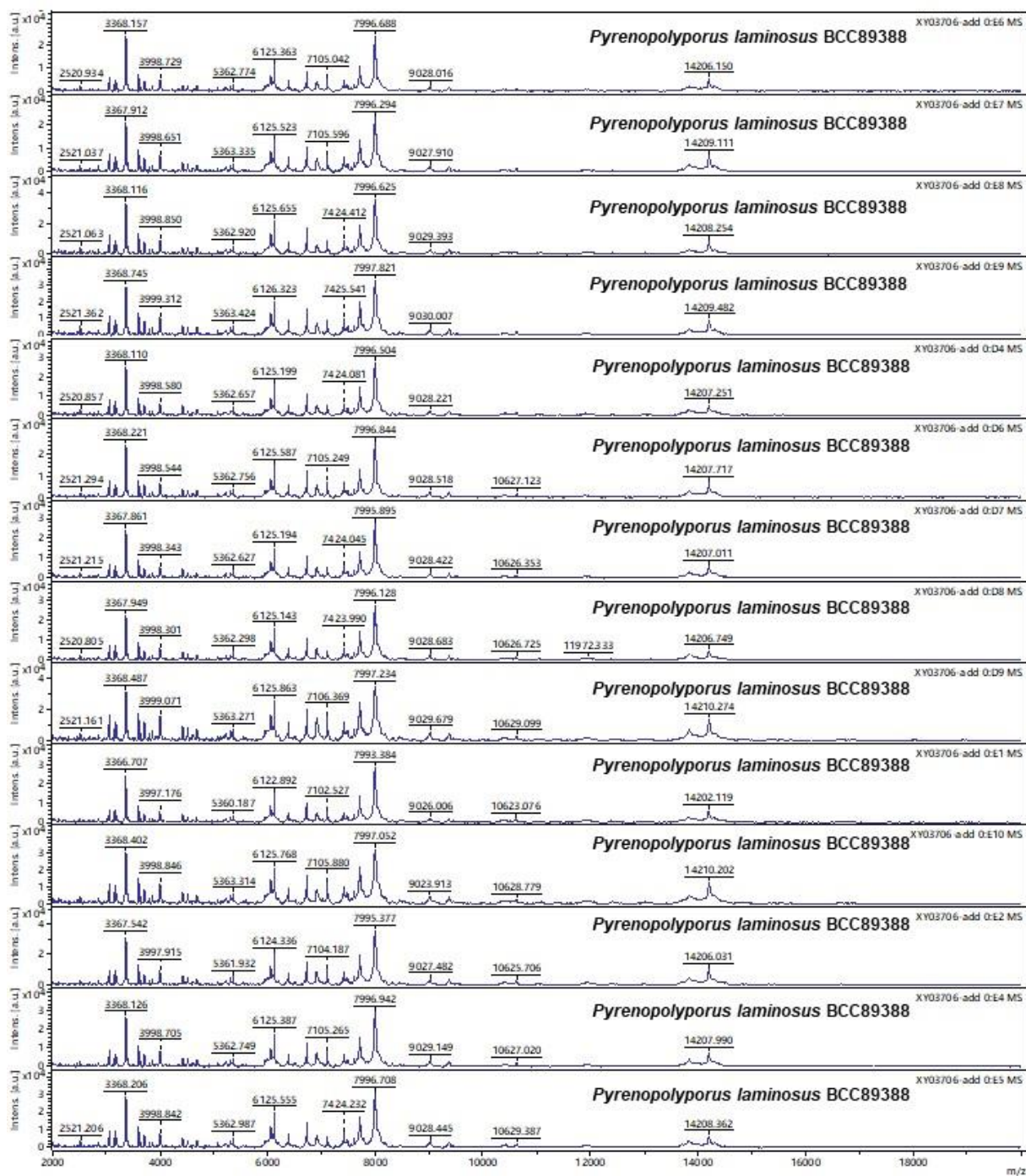


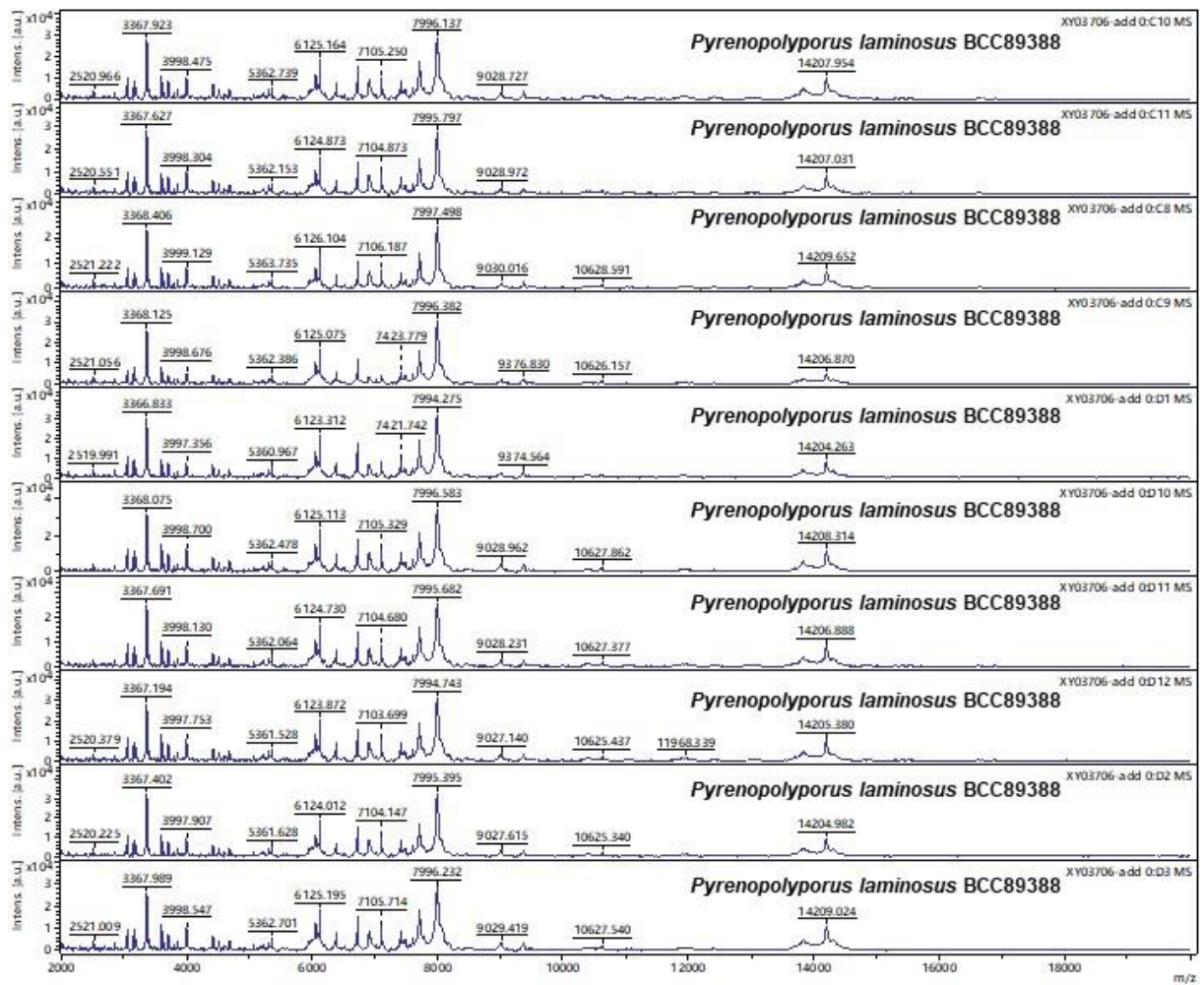




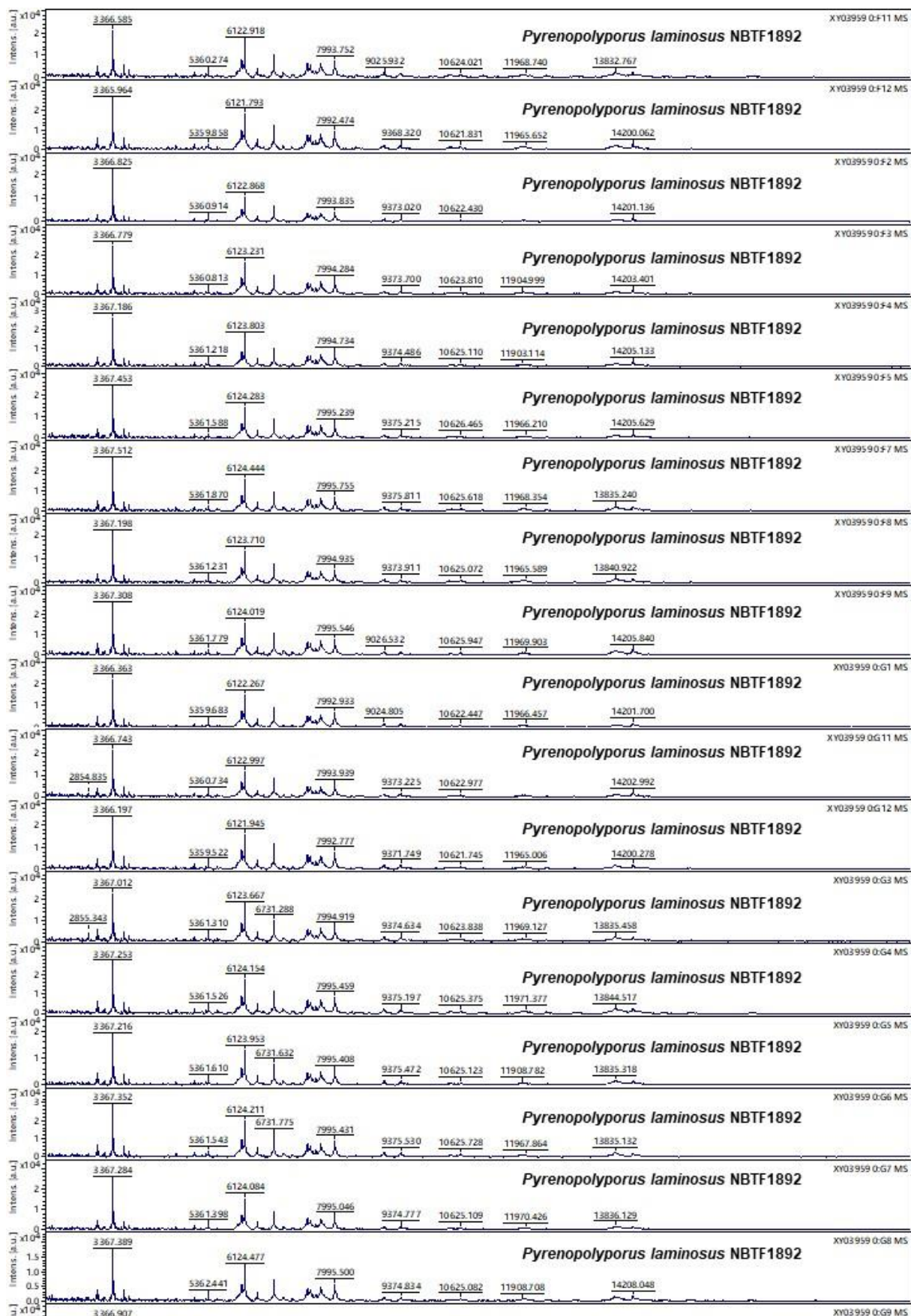


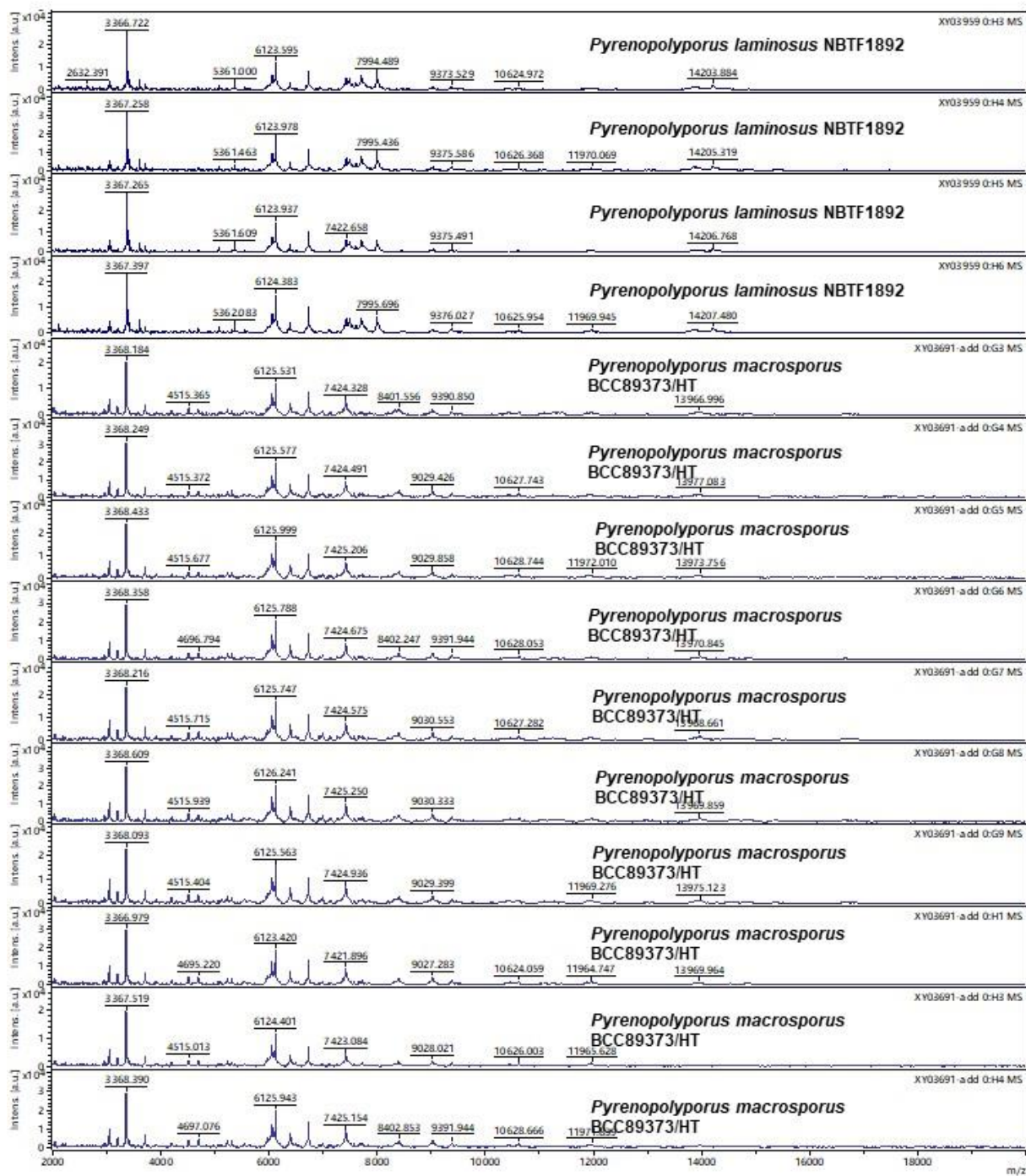




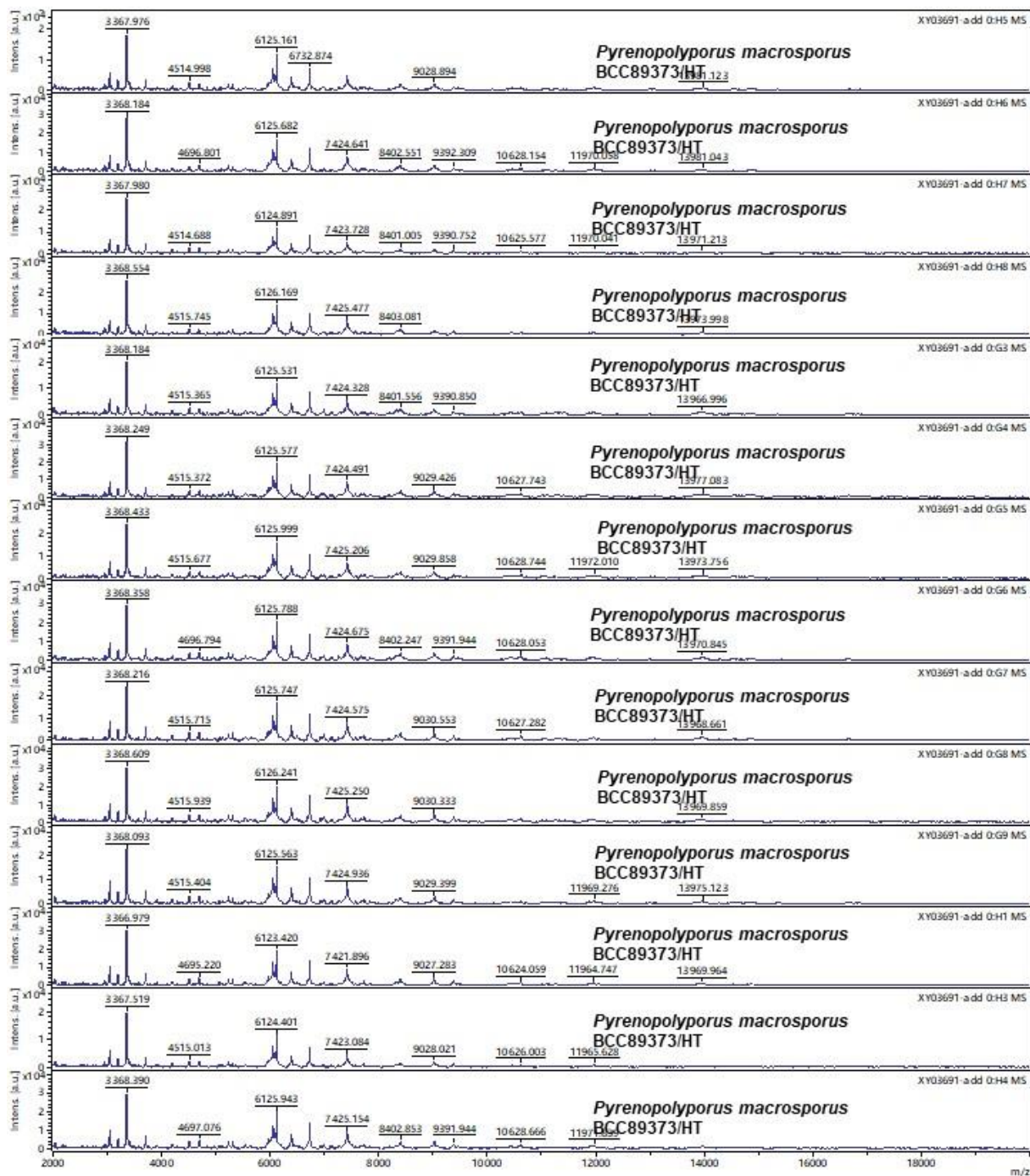




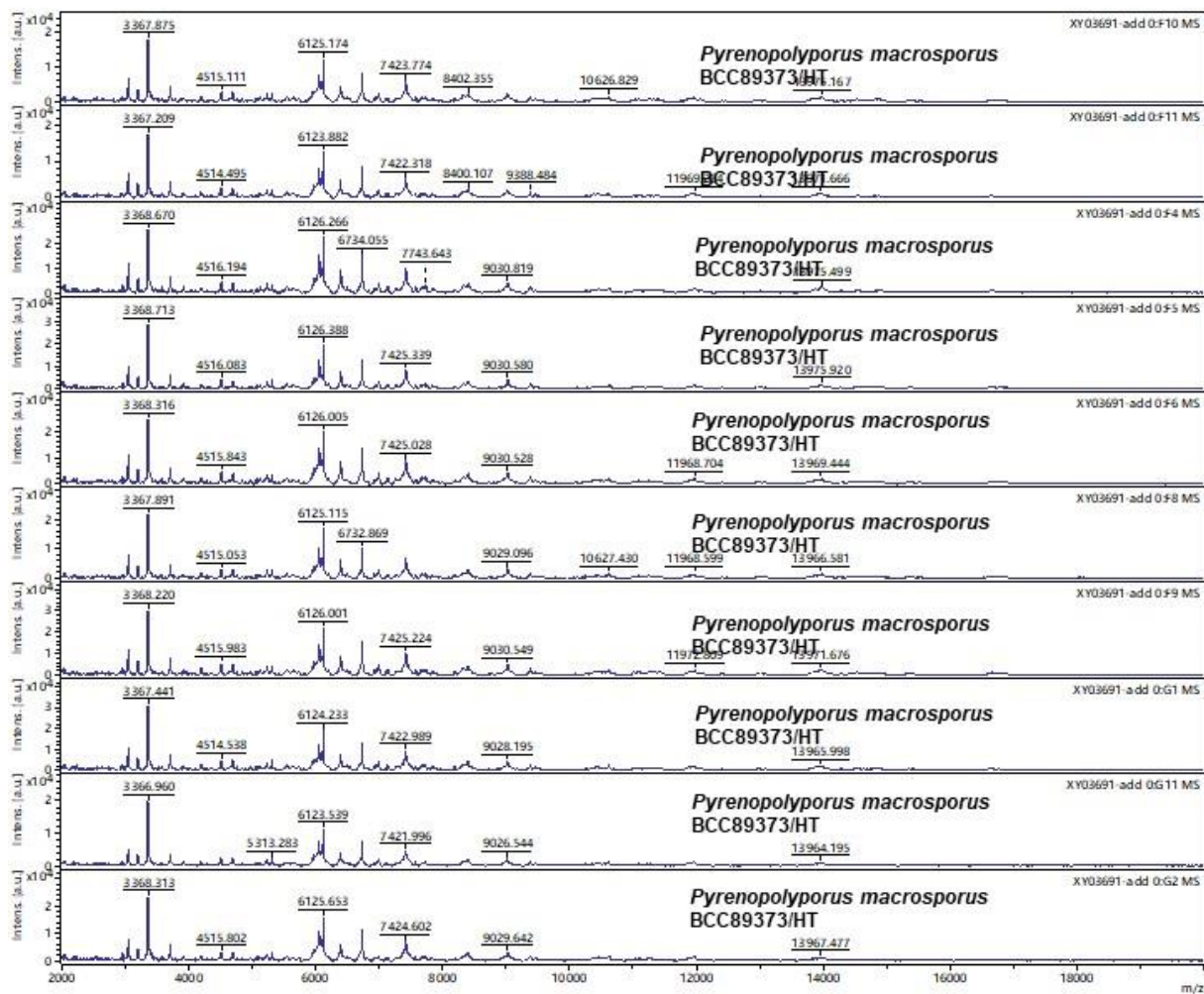


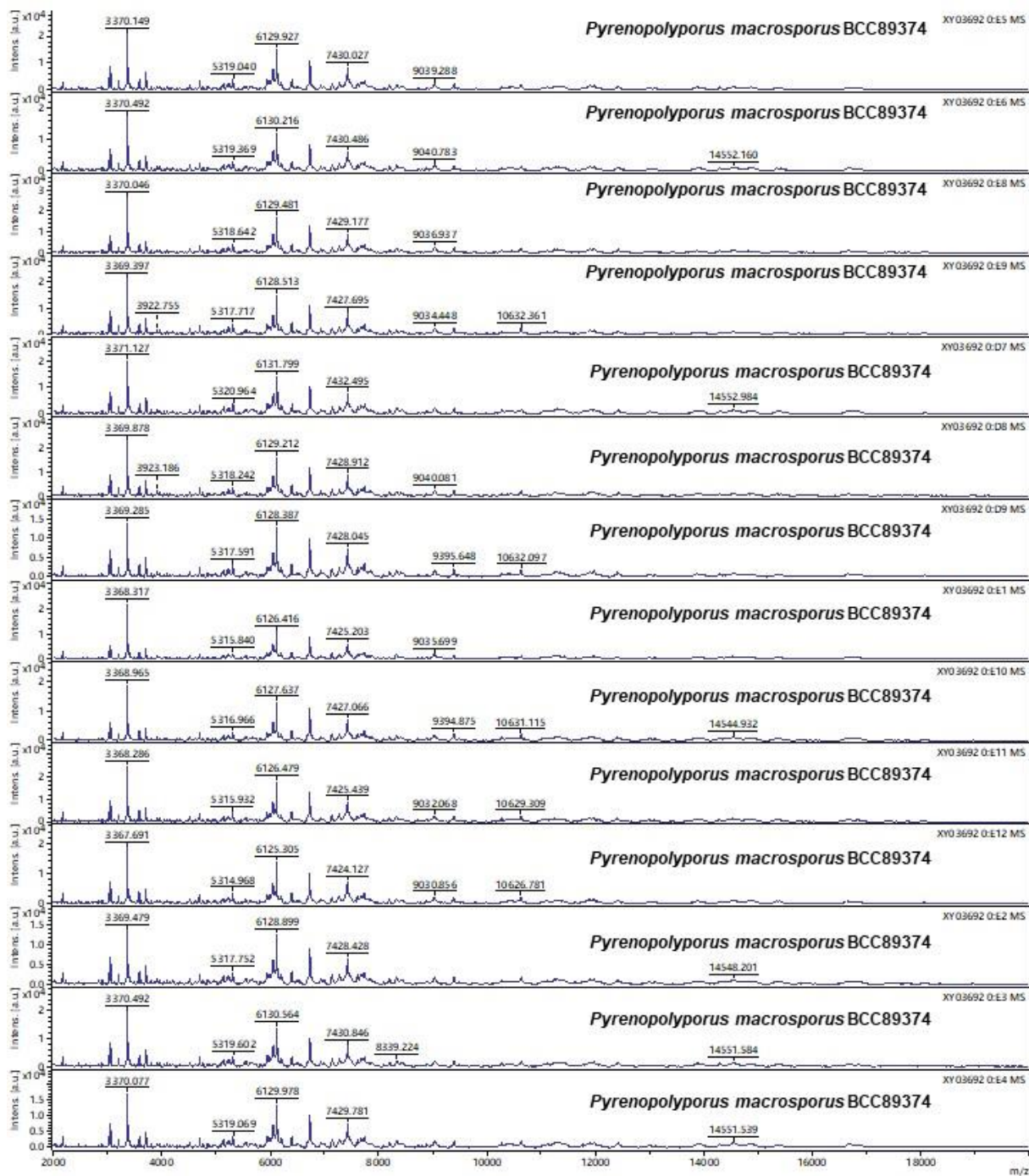


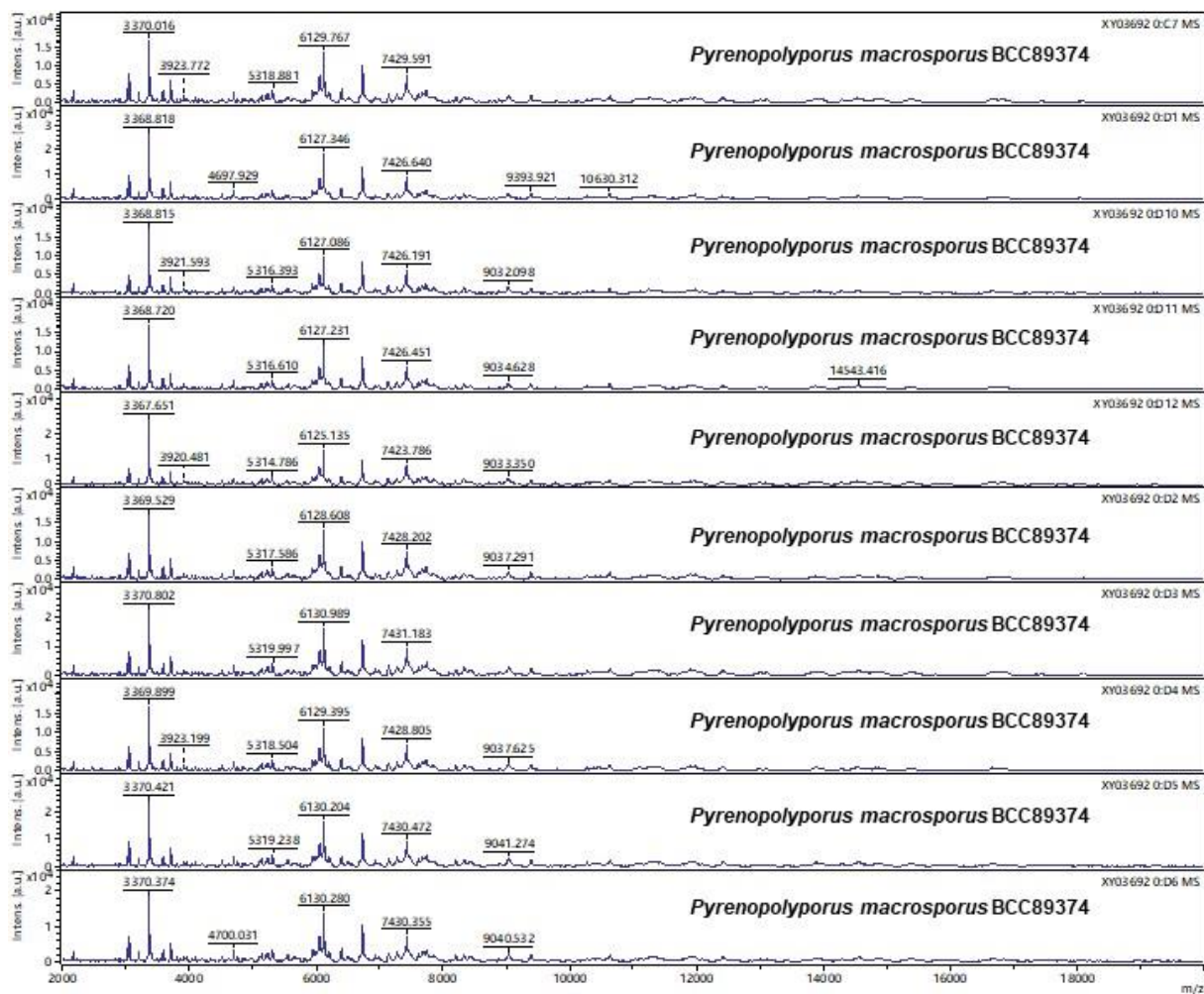




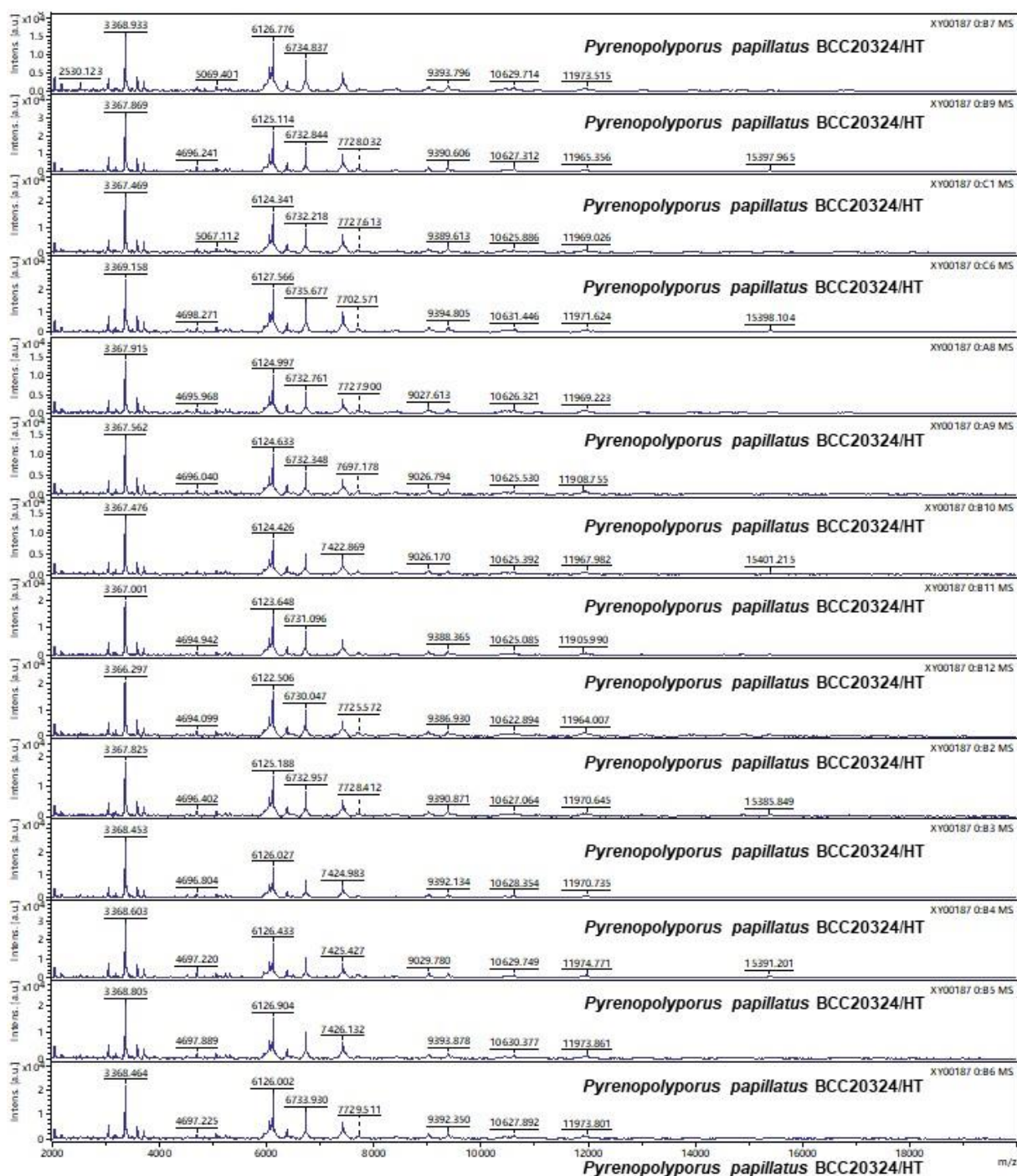


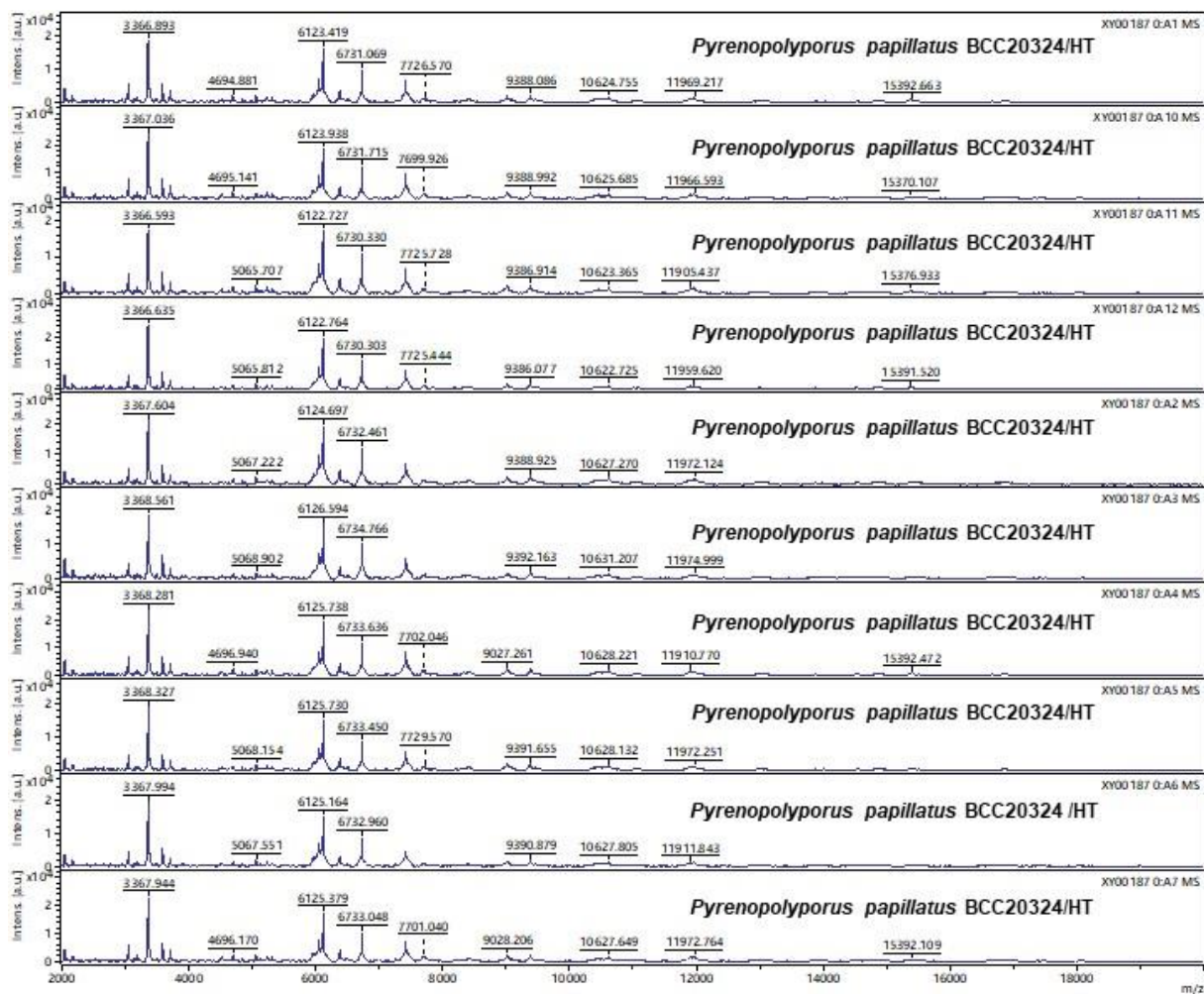


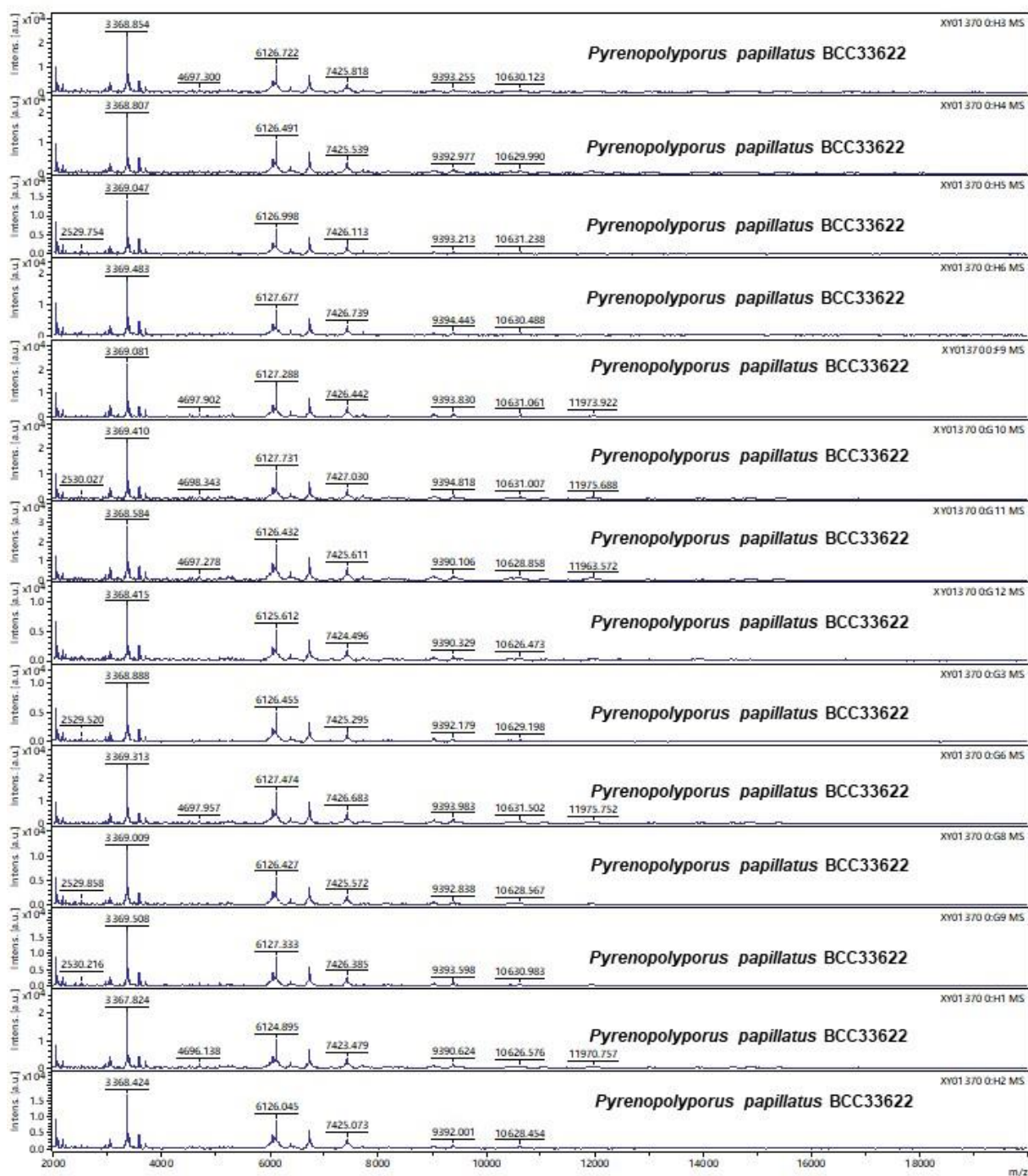




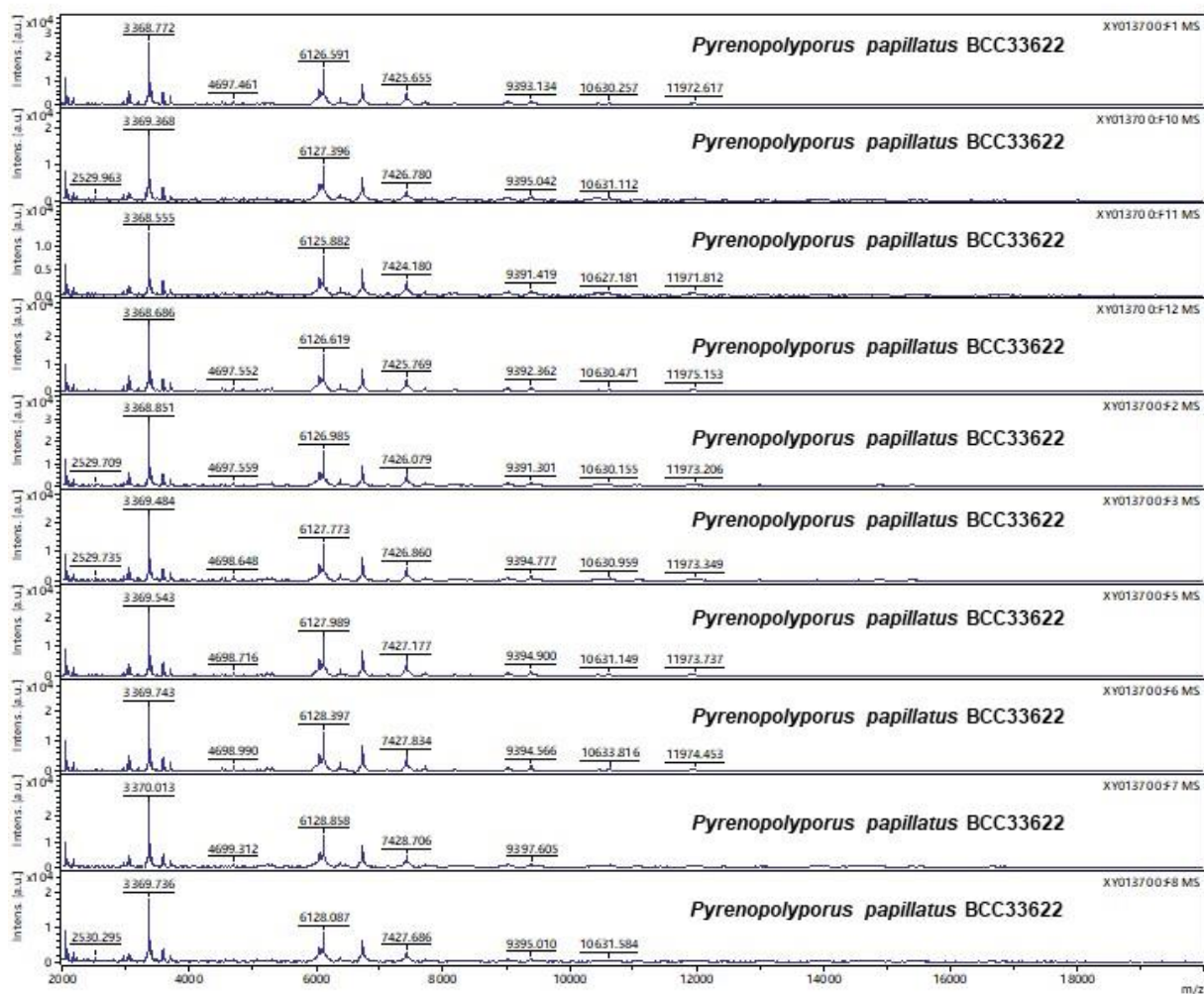


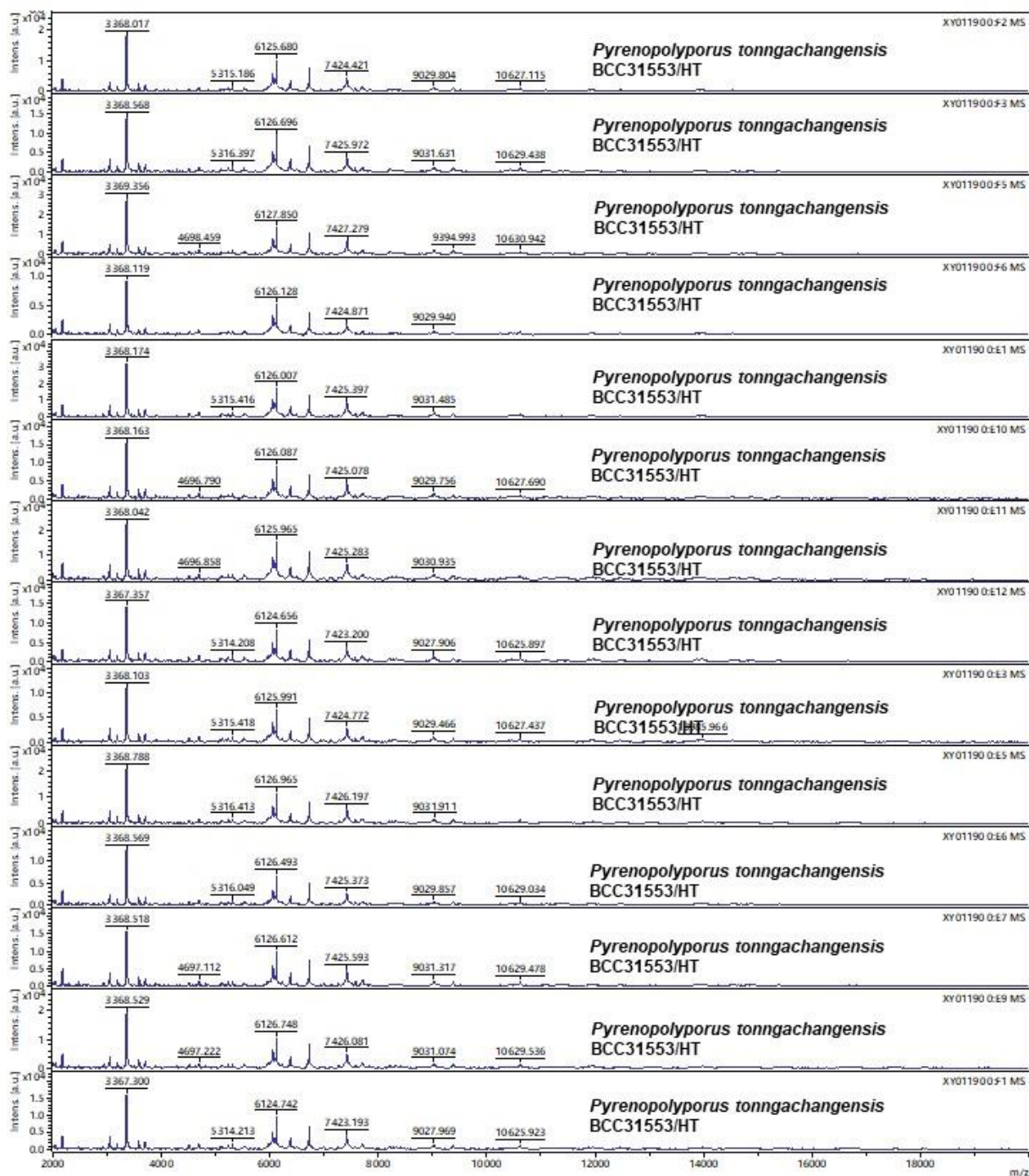


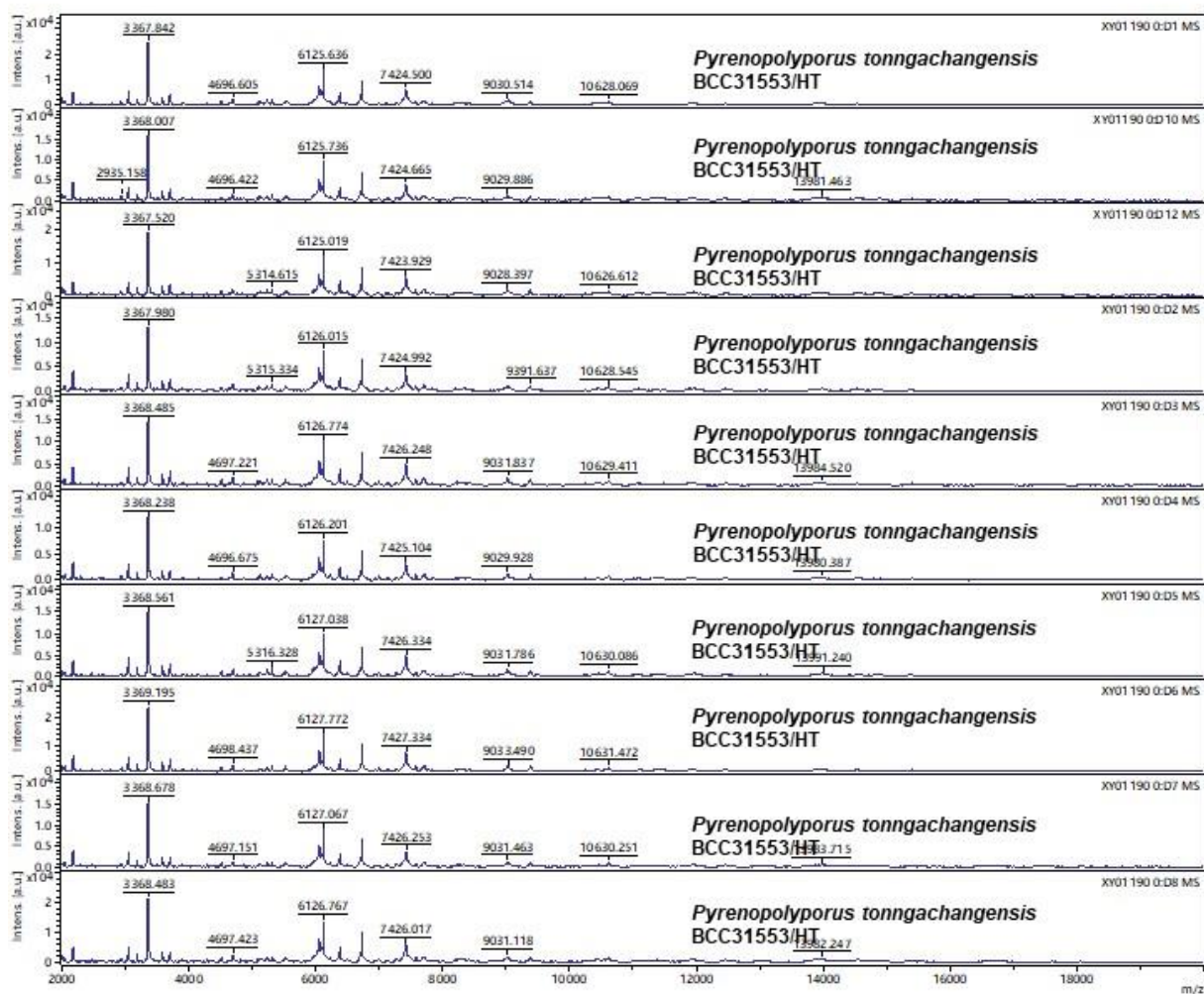




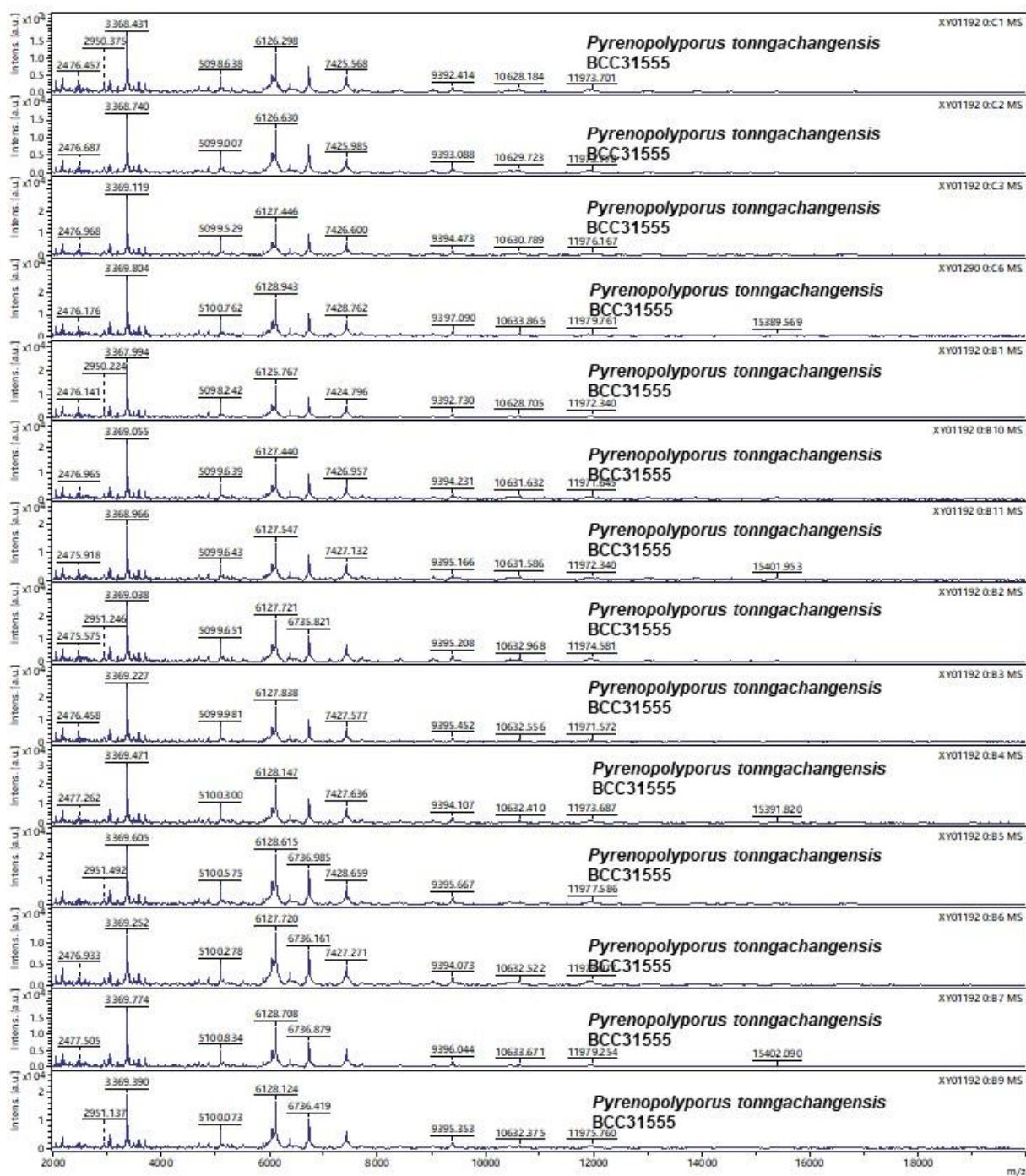


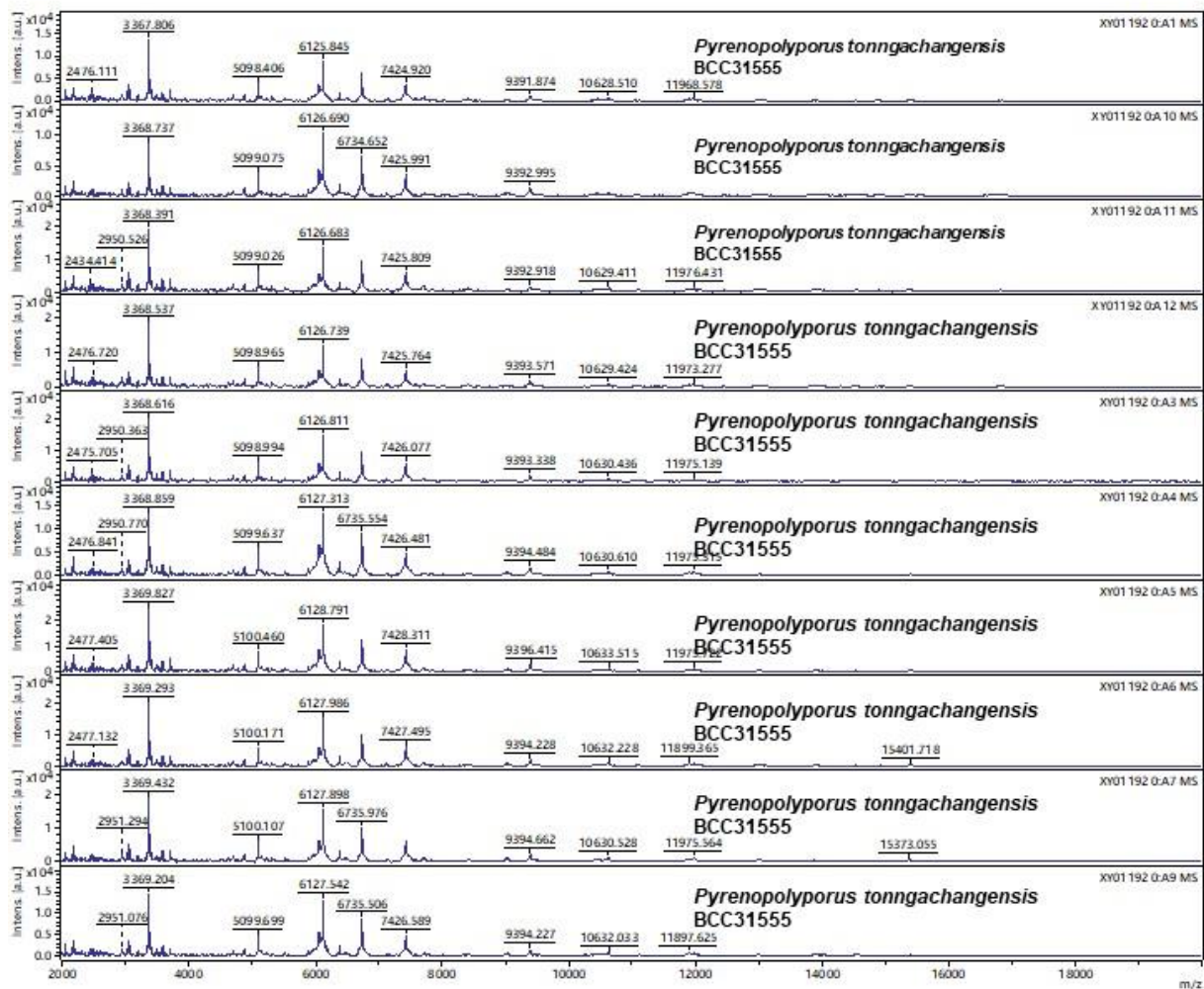


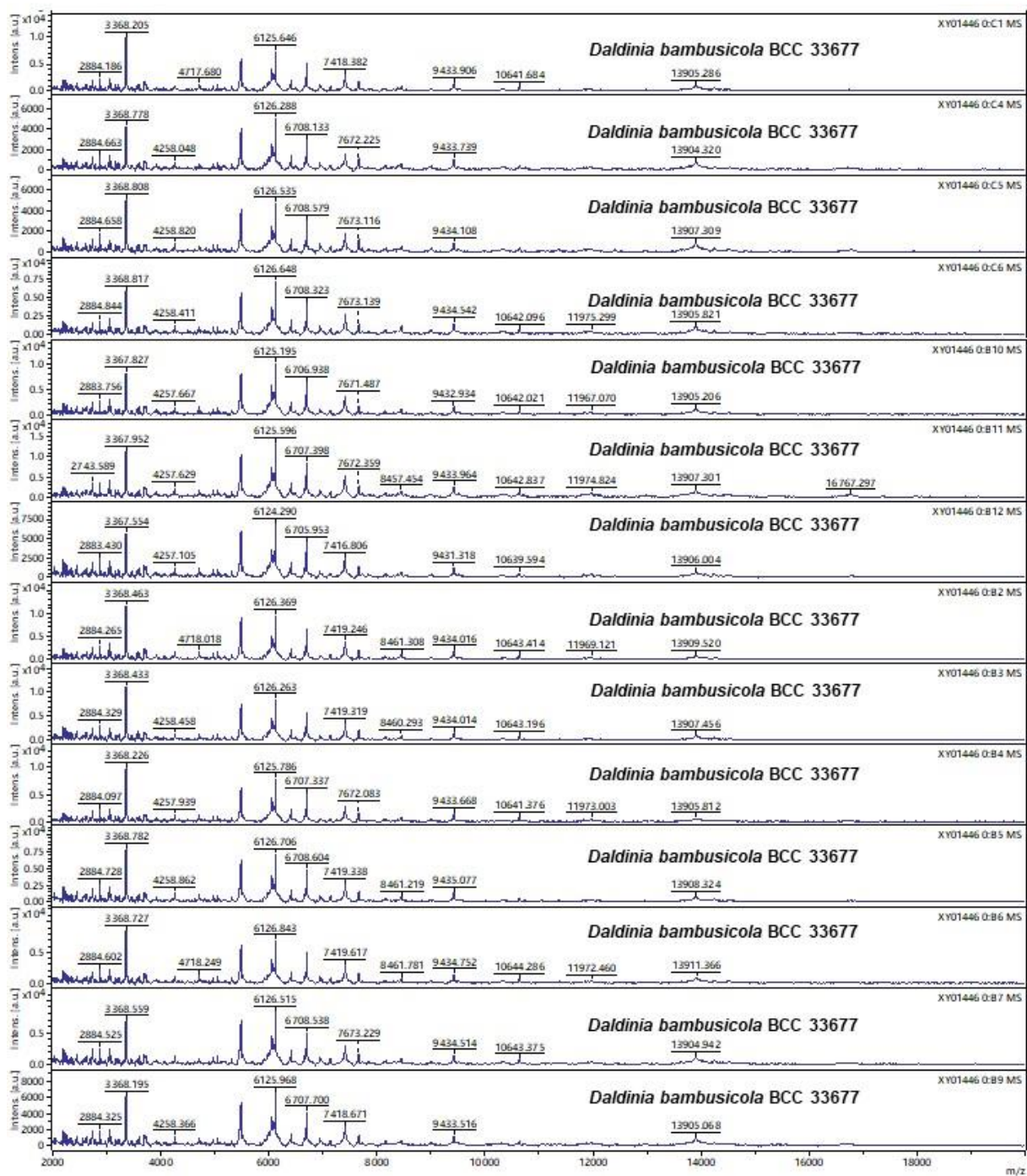




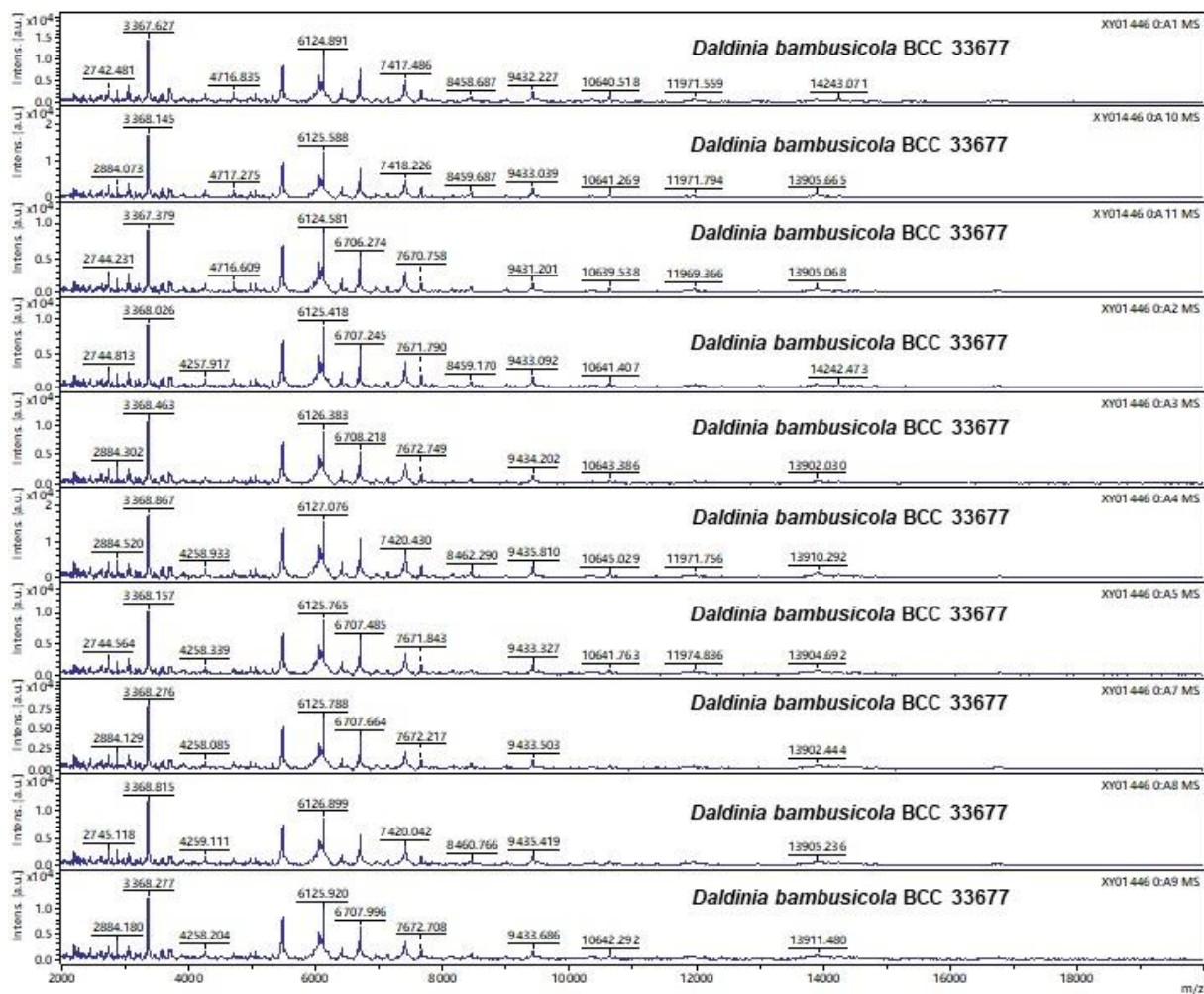


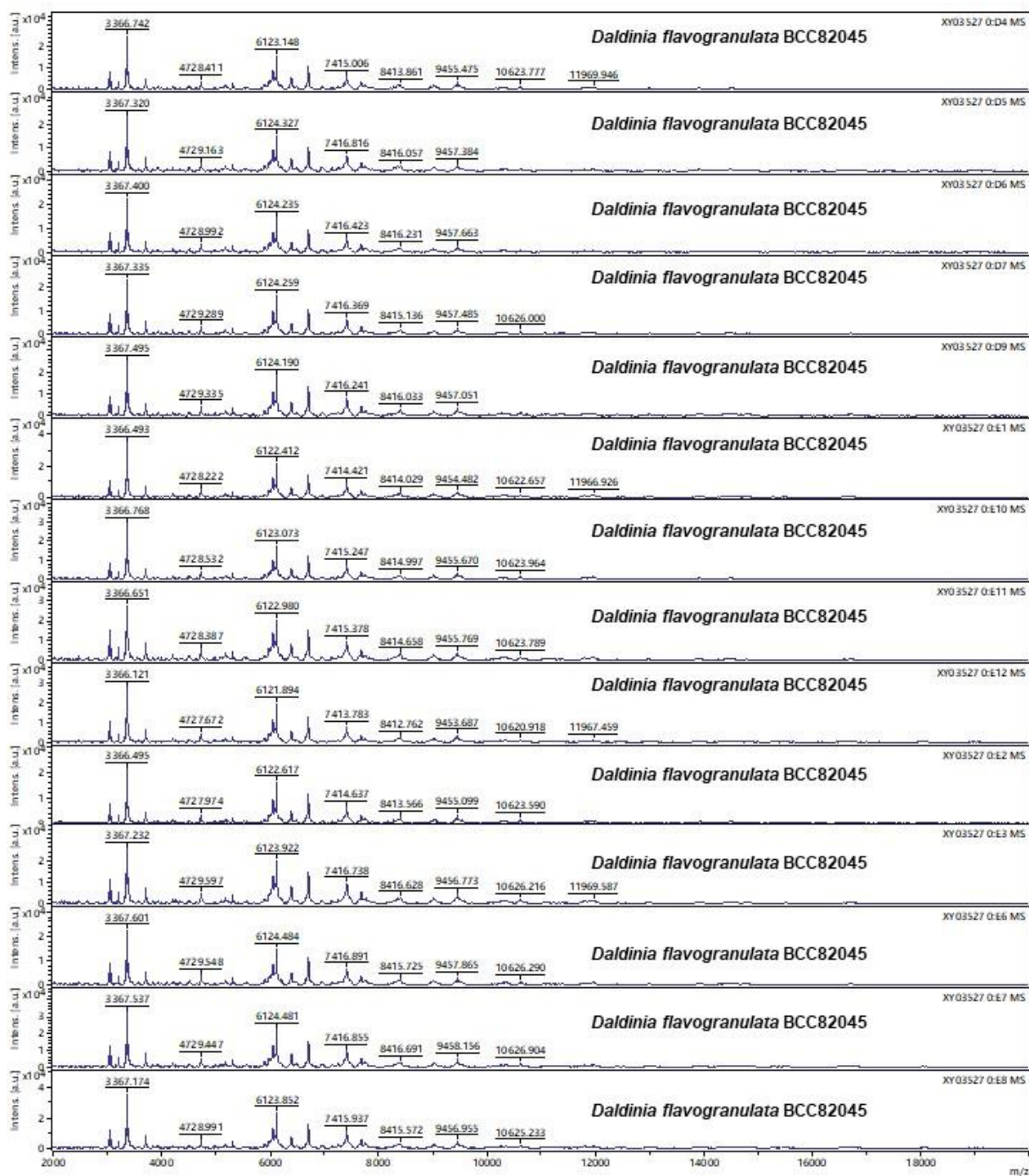


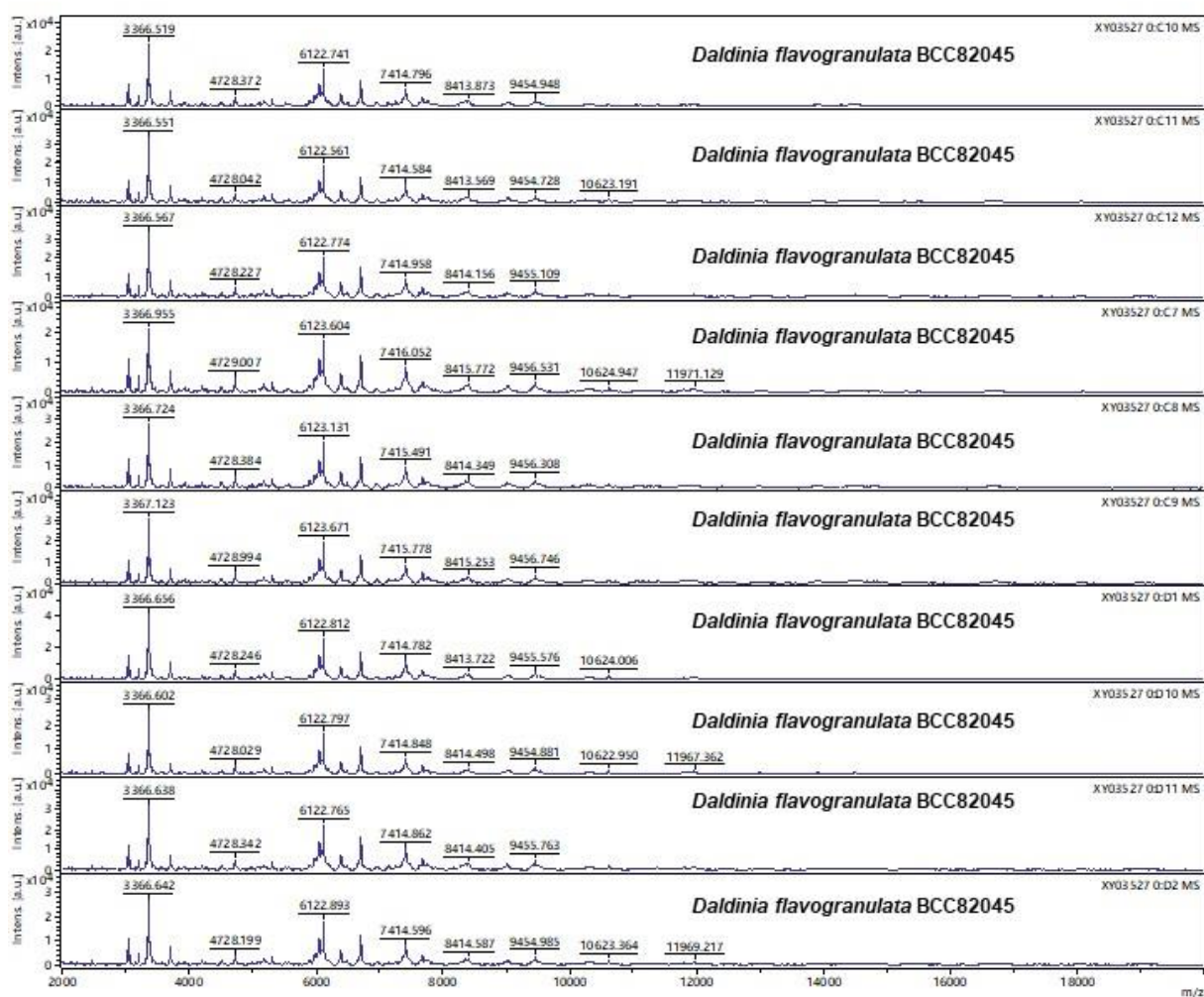




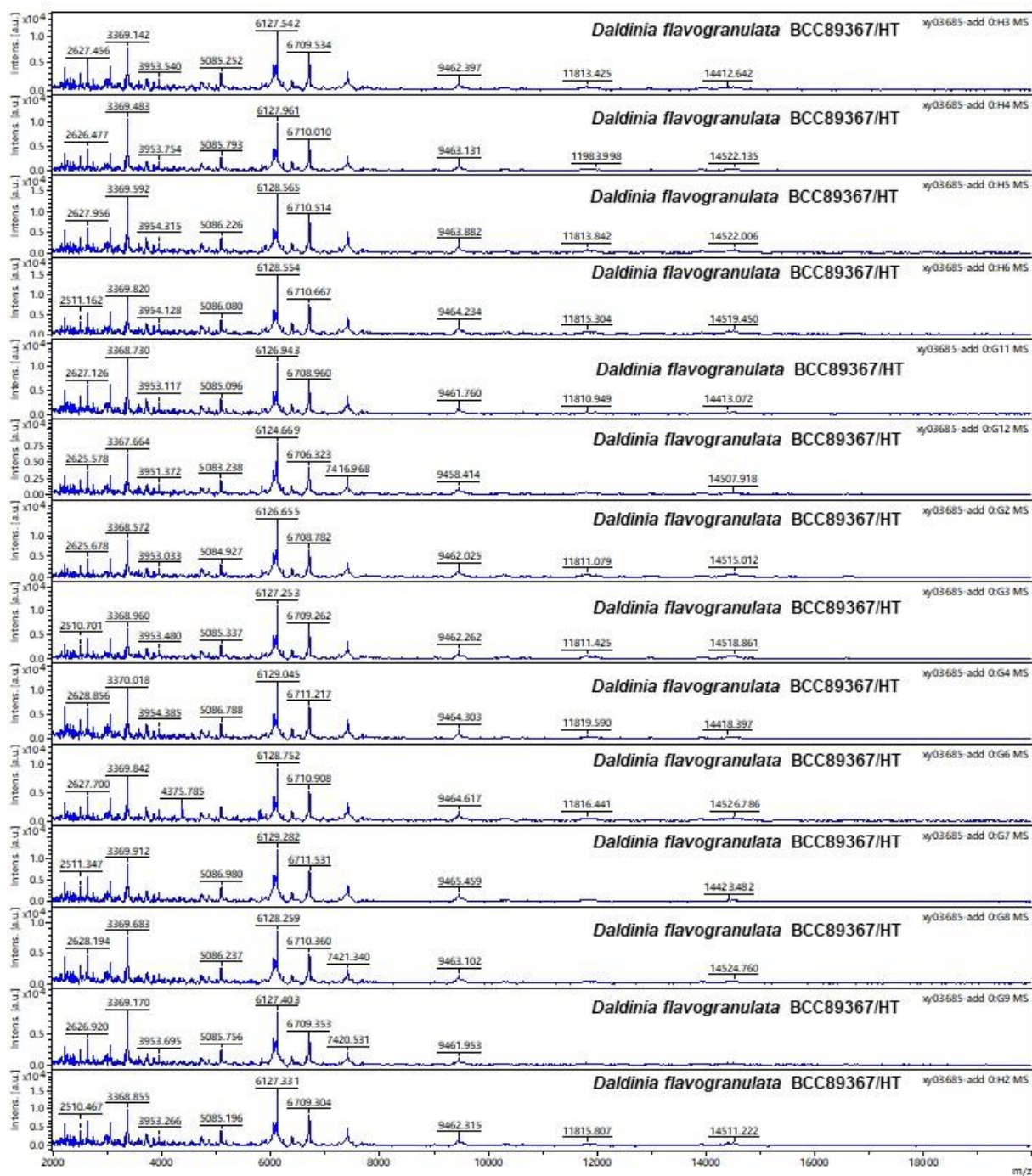












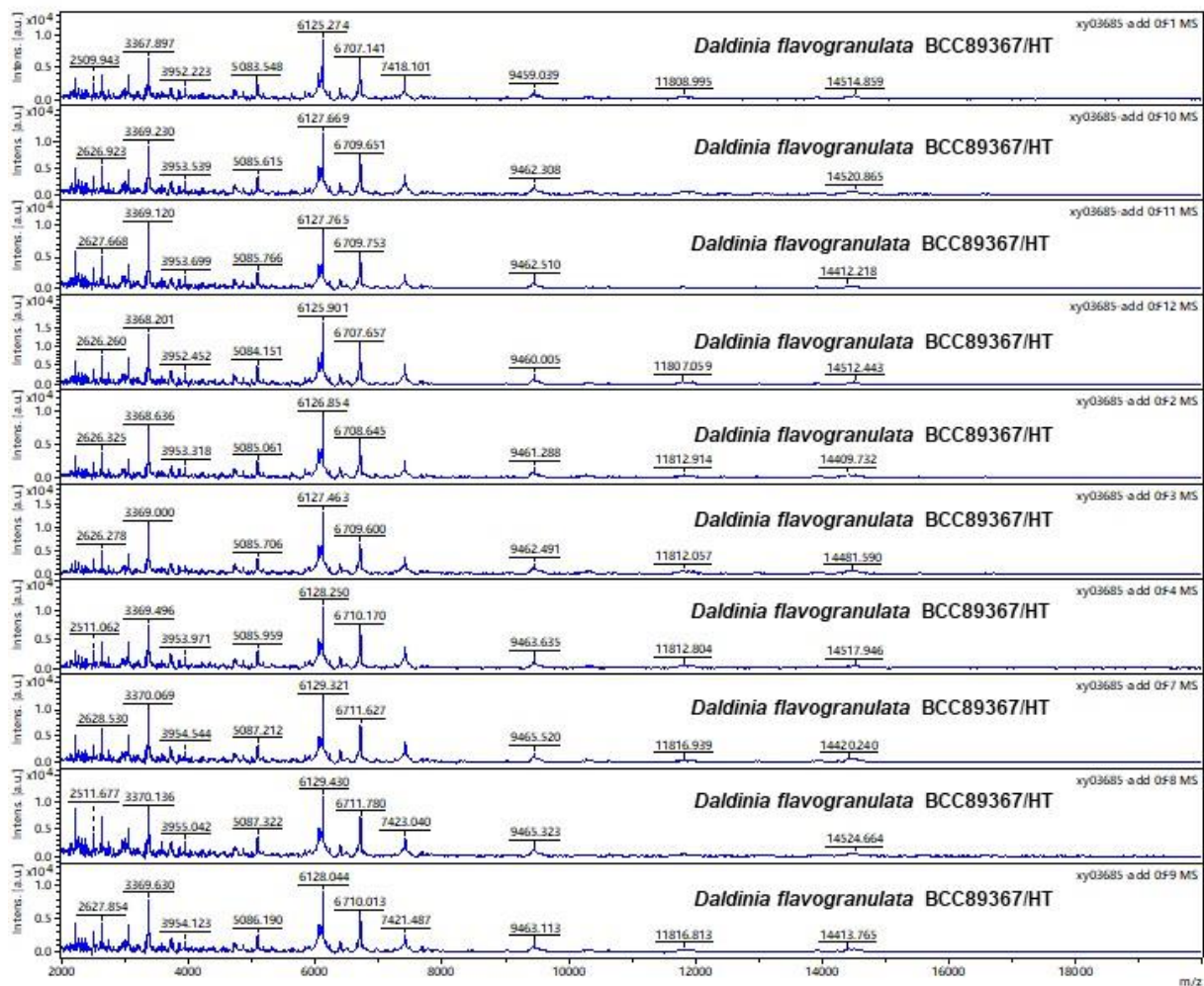


Figure S6. MALDI-TOF MASS SPECTRA.

**Table S1.** Comparison of morphological and chemotaxonomic features of Hypoxylaceae species with massive stroma and long tubular perithecia.

Taxon	Ostioles	Perispore	Germ Slite	Ascospore size ( $\mu\text{m}$ )	KOH-extractable pigments	Metabolites (stroma)
<i>Hypoxylon begae</i>	umbilicate	dehiscent	short, dorsal	21–29 $\times$ 12–14.5	Dense isabelline	BNT, naphthols, and unknown metabolite
<i>Daldinia placentifomis</i>	umbilicate	dehiscent	spore length, dorsal	14.5–16 $\times$ 6.5–7	Olivaceous	BNT, naphthols, naphthoquinones
<i>D. kreztshmarioides</i>	umbilicate	dehiscent	spore length, dorsal	(4) 5–6 $\times$ 13–15(16)	Dark Vinaceous	BNT, Cytochalasan
<i>Pyrenopolyporus laminosus</i>	umbilicate	<b>indehiscent</b>	spore length, dorsal	11–13.5 $\times$ 4.2–4.5	Dilute purple	BNT, naphthols, naphthoquinones
<i>P. hunteri</i>	umbilicate	<b>indehiscent</b>	less than spore length, dorsal	11.5–14 $\times$ 5–5.5	Dense purple or absent	BNT, naphthols, naphthoquinones
<i>P. nicaraguensis</i>	papillate	<b>indehiscent</b>	spore length, dorsal	(11–)12–15(–16) $\times$ 5–6.5	Dilute purple or absent	BNT, naphthols, naphthoquinones
<i>P. tortisporus</i>	umbilicate	<b>indehiscent</b>	spore length, dorsal	9.5–14(–16) $\times$ 4–6	Dense amber or Olivaceous	BNT, naphthols, naphthoquinones
<i>P. symphyon</i>	papillate	<b>indehiscent</b>	spore length, dorsal	9.5–12(–13) $\times$ 4–5	Purple or absent	BNT, naphthols, naphthoquinones, daldinal A, daldinal C
<i>P. laminosus</i> (this study)	umbilicate	<b>indehiscent</b>	spore length, dorsal	(12–)13–14(–15) $\times$ 4–5	Dense purple	BNT, hypoxylones
<i>P. bambusicola</i> (this study)	umbilicate	<b>indehiscent</b>	spore length, dorsal	8–10(–11) $\times$ (3–) 4–5	Dense purple	BNT, hypoxylones
<i>P. macrosporus</i> (this study)	inconspicuous	<b>indehiscent</b>	spore length, dorsal	(14–) 16–17 $\times$ (6–)7–8	Dense purple	BNT, hypoxylones
<i>P. papillatus</i> (this study)	papillate	<b>indehiscent</b>	spore length, dorsal	(11–) 12–13(–14) $\times$ 4–5	Dense purple	BNT, hypoxylones
<i>P. tonngachangensi</i> (this study)	umbilicate	<b>indehiscent</b>	2/3 spore length, dorsal	(12–) 13–14(–16) $\times$ 4–5	Dense purple	BNT, hypoxylones
<i>P. cinereopigmentosus</i> (this study)	inconspicuous	<b>indehiscent</b>	spore length, dorsal	(12–) 13–14 (–15) $\times$ 6–7	Grey	BNT, hypoxylones



**Table S2.** Dereplicated metabolites from the stromatal extracts of the *Pyrenopolyporus* spp. and in-house standards.

Compound	<i>m/z</i>	rt	CCS	Formula	Annotation*
Hypoaxylone (1)	333.07588 [M+H] <sup>+</sup>	13.42	169.2	C <sub>20</sub> H <sub>12</sub> O <sub>5</sub>	Level 2
BNT (2)	319.09643 [M+H] <sup>+</sup>	12.28	172.6	C <sub>20</sub> H <sub>14</sub> O <sub>4</sub>	Level 1
3	349.07041 [M+H] <sup>+</sup>	11.38	175.1	C <sub>20</sub> H <sub>12</sub> O <sub>6</sub>	Level 2
4	258.10997 [M+Na] <sup>+</sup>	8.92	159.3	C <sub>13</sub> H <sub>17</sub> NO <sub>3</sub>	n.i.
5	633.45371 [M+H] <sup>+</sup>	18.59	251.9	C <sub>30</sub> H <sub>60</sub> N <sub>6</sub> O <sub>8</sub>	n.i.

\*Level 0 corresponds to data obtained from in-house standards; level 1 to annotations by comparison with standards; level 2 to putative annotations (i.e., MS/MS library search); level 3 to a compound class assignment; n.i. to non-identified metabolites. rt = retention time in min; CCS = collisional cross section in Å<sup>2</sup>.

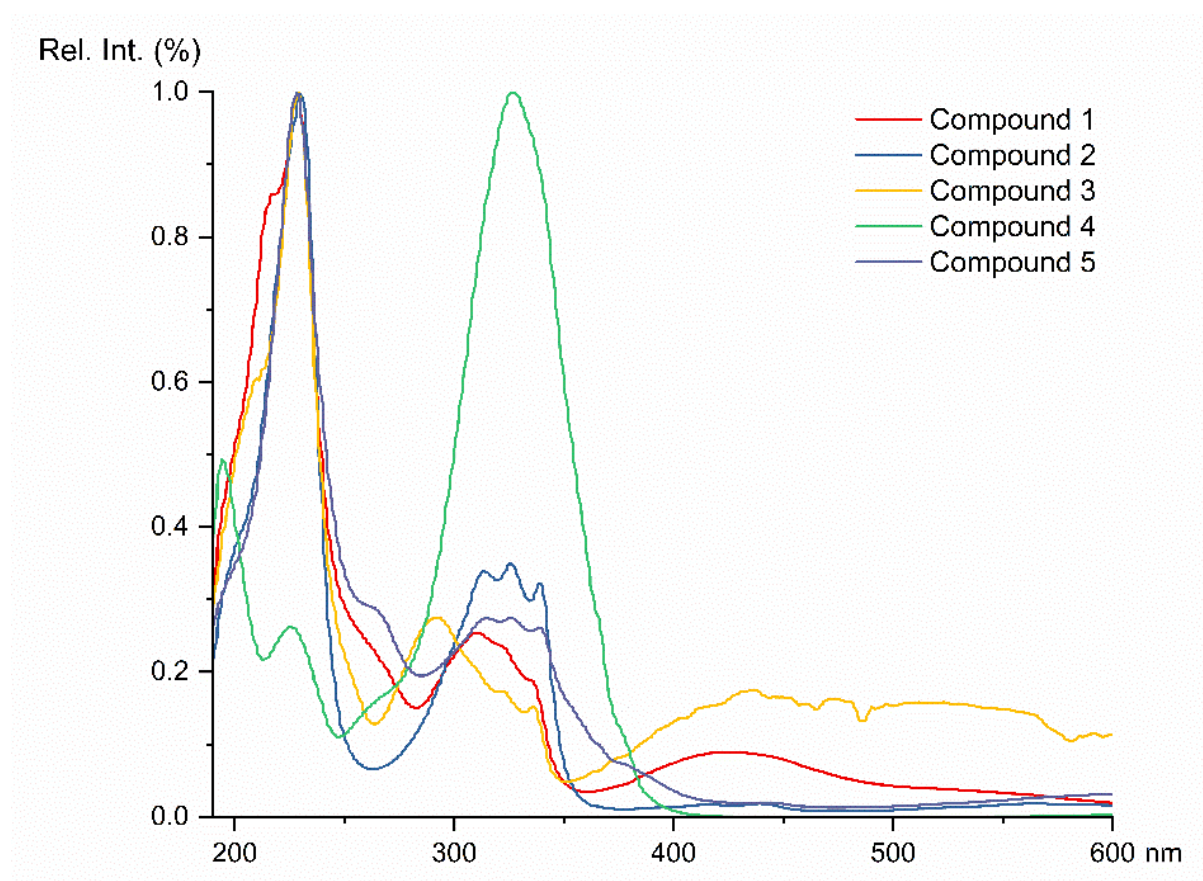


**Figure S7.** DAD spectra of the major metabolites (1–5) depicted in the stromata of the evaluated *Pyrenopolyporus* spp.

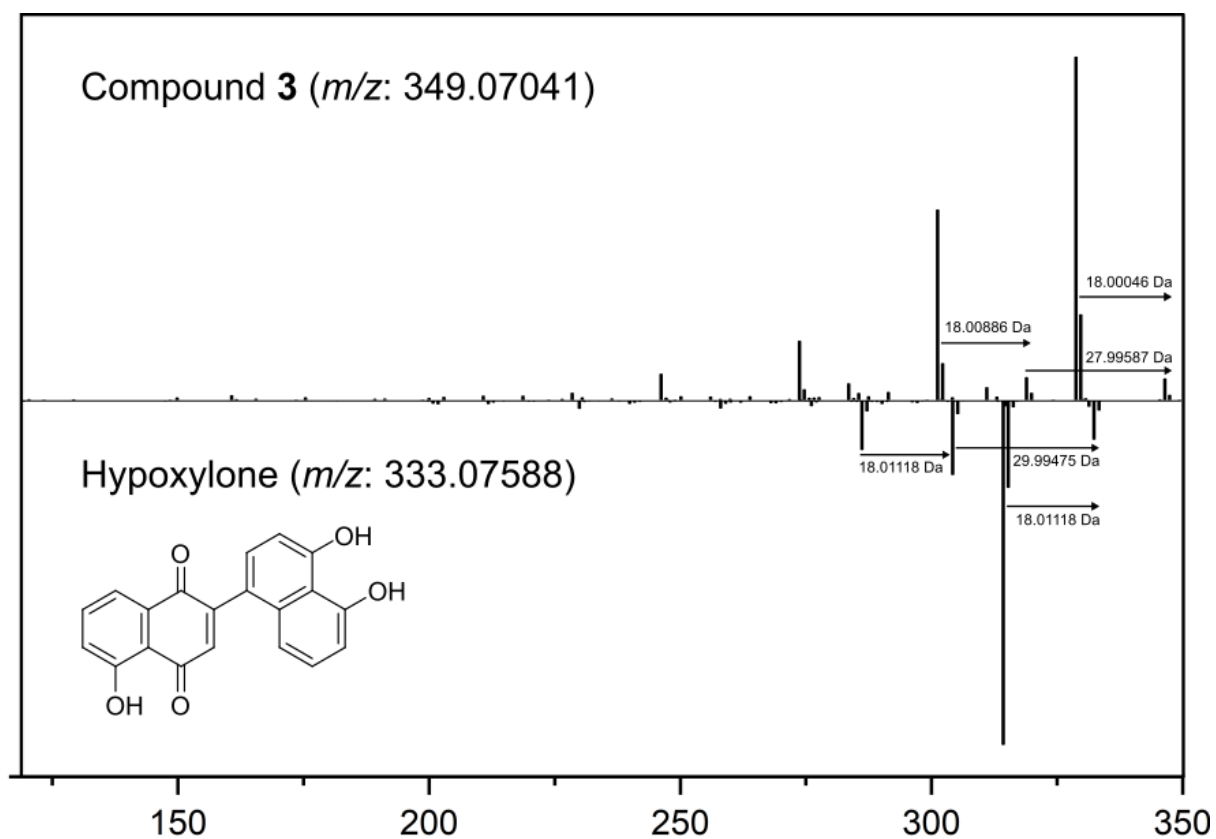


**Figure S8.** MS/MS spectra comparison between hypoxylone (**1**) and compound **3**. The MS/MS similarity score between the two metabolites is < 500, but both spectra share analogous neutral losses for the major fragment ions.